Behavioral/Cognitive

Diacylglycerol Lipase-Alpha Regulates Hippocampal-Dependent Learning and Memory Processes in Mice

Lesley D. Schurman,[1] Moriah C. Carper,[1] Lauren V. Moncayo,[1] Daisuke Ogasawara,[2] Karen Richardson,[1] Laikang Yu,[3] Xiaojie Liu,[3] Justin L. Poklis,[1] Qing-Song Liu,[3] Benjamin F. Cravatt,[2] and Aron H. Lichtman[1,4]

[1]Department of Pharmacology and Toxicology, Virginia Commonwealth University, Richmond, Virginia 23298, [2]Department of Molecular Medicine, Scripps Research Institute, La Jolla, California 92037, [3]Department of Pharmacology and Toxicology, Medical College of Wisconsin, Milwaukee, Wisconsin 53226, and [4]Department of Medicinal Chemistry, Virginia Commonwealth University, Richmond, Virginia 23298

Diacylglycerol lipase-α (DAGL-α), the principal biosynthetic enzyme of the endogenous cannabinoid 2-arachidonylglycerol (2-AG) on neurons, plays a key role in CB_1 receptor-mediated synaptic plasticity and hippocampal neurogenesis, but its contribution to global hippocampal-mediated processes remains unknown. Thus, the present study examines the role that DAGL-α plays on LTP in hippocampus, as well as in hippocampal-dependent spatial learning and memory tasks, and on the production of endocannabinoid and related lipids through the use of complementary pharmacologic and genetic approaches to disrupt this enzyme in male mice. Here we show that DAGL-α gene deletion or pharmacological inhibition disrupts LTP in CA1 of the hippocampus but elicits varying magnitudes of behavioral learning and memory deficits in mice. In particular, *DAGL-*$\boldsymbol{\alpha}^{-/-}$ mice display profound impairments in the Object Location assay and Morris Water Maze (MWM) acquisition engaging in nonspatial search strategies. In contrast, WT mice administered the DAGL-α inhibitor DO34 show delays in MWM acquisition and reversal learning, but no deficits in expression, extinction, forgetting, or perseveration processes in this task, as well as no impairment in Object Location. The deficits in synaptic plasticity and MWM performance occur in concert with decreased 2-AG and its major lipid metabolite (arachidonic acid), but increases of a 2-AG diacylglycerol precursor in hippocampus, PFC, striatum, and cerebellum. These novel behavioral and electrophysiological results implicate a direct and perhaps selective role of DAGL-α in the integration of new spatial information.

Key words: 2-arachidonylglycerol; diacylglycerol lipase; endocannabinoid; endogenous cannabinoid; LTP; Morris water maze

Significance Statement

Here we show that genetic deletion or pharmacologic inhibition of diacylglycerol lipase-α (DAGL-α) impairs hippocampal CA1 LTP, differentially disrupts spatial learning and memory performance in Morris water maze (MWM) and Object Location tasks, and alters brain levels of endocannabinoids and related lipids. Whereas *DAGL-*$\boldsymbol{\alpha}^{-/-}$ mice exhibit profound phenotypic spatial memory deficits, a DAGL inhibitor selectively impairs the integration of new information in MWM acquisition and reversal tasks, but not memory processes of expression, extinction, forgetting, or perseveration, and does not affect performance in the Objection Location task. The findings that constitutive or short-term DAGL-α disruption impairs learning and memory at electrophysiological and selective *in vivo* levels implicate this enzyme as playing a key role in the integration of new spatial information.

Introduction

A growing body of evidence implicates the importance of 2-arachidonoyl glycerol (2-AG), the most highly expressed endogenous cannabinoid in brain, in regulating learning and memory. Diacylglycerol lipase (DAGL) forms 2-AG through the hydrolysis of diacylglycerols (Chau and Tai, 1981; Okazaki et al., 1981) and exists as two distinct biosynthetic enzymes, DAGL-α and DAGL-β (Bisogno et al., 2003), which are expressed on distinct cell types, as well as in brain areas important for learning and

Received May 27, 2018; revised April 24, 2019; accepted May 11, 2019.

Author contributions: L.D.S., Q.-S.L., B.F.C., and A.H.L. designed research; L.D.S., M.C.C., L.V.M., K.R., L.Y., X.L., J.L.P., and Q.-S.L. performed research; L.D.S. and Q.-S.L. analyzed data; L.D.S. wrote the first draft of the paper; L.D.S., J.L.P., and Q.-S.L. wrote the paper; D.O. and B.F.C. contributed unpublished reagents/analytic tools; Q.-S.L., B.F.C., and A.H.L. edited the paper.

This work was supported by the National Institutes of Health Grants NS093990 and DA039942 to A.H.L., Grant 1F31NS095628–01A1 to L.D.S., Grant DA035217 to Q.-S.L., Grant DA033760 to B.F.C., and Center Grant P30DA033934. This work was also supported by Virginia Commonwealth University School of Pharmacy start-up funds. The content is solely the responsibility of the authors and does not necessarily represent the official views of the National Institutes of Health.

The authors declare no competing financial interests.

Correspondence should be addressed to Aron H. Lichtman at aron.lichtman@vcuhealth.org.

https://doi.org/10.1523/JNEUROSCI.1353-18.2019

memory (Katona et al., 2006; Lafourcade et al., 2007). Within the CNS, DAGL-β is highly expressed on microglia, whereas DAGL-α, expressed on synapse-rich plasma membranes of dendritic spines (Yoshida et al., 2006), serves as the principal synthetic enzyme of 2-AG on neurons (Viader et al., 2015).

DAGL-α modulates neurotransmission through distinct processes of neurogenesis and endocannabinoid-mediated short-term synaptic plasticity, implicating it in learning and memory processes. Adult neurogenesis represents a form of cellular plasticity in the developed brain. Two prominent brain areas showing adult neurogenesis, the subventricular zone and the hippocampus, which express high levels of DAGL-α (Goncalves et al., 2008), undergo marked reductions in the proliferation of neuronal progenitor cells in *DAGL-α*$^{-/-}$ mice (Gao et al., 2010). Similarly, the nonselective DAGL inhibitors RHC80267 and tetrahydrolipstatin reduce proliferation of neuronal progenitor cells in the subventricular zone (Goncalves et al., 2008). DAGL-α also plays an essential role in endocannabinoid-mediated retrograde synaptic suppression in which 2-AG synthesized at postsynaptic terminals acts as a retrograde messenger to activate the presynaptic cannabinoid receptor Type 1 (CB_1), which inhibits synaptic transmission. Tanimura et al. (2010), reported that deletion of DAGL-α, but not DAGL-β, annihilated two forms of endocannabinoid-mediated short-term synaptic plasticity, depolarization-induced suppression of excitation (DSE) and inhibition (DSI) in hippocampus, striatum, and cerebellum. Similarly, Gao et al. (2010) replicated these findings in hippocampus, and Yoshino et al. (2011) reported that DAGL-α plays a necessary role in DSI in the PFC. Furthermore, the DAGL inhibitor DO34 blocked DSE in cerebellar slices and DSI in hippocampal slices in a concentration-dependent manner (Ogasawara et al., 2016).

The cell signaling events that occur after learning are frequently studied in terms of LTP. Carlson et al. (2002) demonstrated that transient release of endocannabinoids by depolarization facilitated the induction of LTP when preceded by DSI, suggesting that endocannabinoids may enhance plasticity at Schaffer collateral-CA1 synapses through a disinhibitory action. However, the role that the major 2-AG biosynthetic enzyme DAGL-α plays in the induction of LTP remains unknown. Here we hypothesize that this enzyme plays a necessary role in the induction of LTP. Accordingly, we predict that pharmacological inhibition or genetic deletion of DAGL-α will disrupt LTP.

The present study also investigated the *in vivo* role of DAGL-α in spatial learning and memory tasks. Specifically, we evaluated whether endocannabinoid-regulated short-term synaptic plasticity disruption by DAGL-α deletion or inhibition translates to hippocampal-dependent learning and memory task deficits in the Morris Water Maze (MWM) and Object Location (OL) assays. Given the important role of hippocampal neurogenesis in the processing of spatial memory (Lieberwirth et al., 2016), we investigated the consequences of DAGL-α disruption on spatial memory processes of acquisition, expression, extinction, forgetting, reversal, and perseveration in the MWM. To circumvent known pitfalls related to constitutive genetic deletions, such as the role of DAGL-α in axonal guidance during development (Williams et al., 2003), we used the DAGL-α/β inhibitor, DO34, and *DAGL-α*$^{-/-}$ mice. Because DO34 also inhibits other serine hydrolases (i.e., ABHD2, ABHD6, CES1C, PLA2G7, PAFAH2), we evaluated DO53, a structural analog of DO34 that cross-reacts with these off-targets but does not inhibit DAGL (Ogasawara et al., 2016).

In the present study, we ascertain the consequences of DAGL-α disruption at three levels of investigation: cellular responses to LTP, *in vivo* spatial learning and memory tasks, and alterations of endocannabinoid lipids, their substrates, and metabolites, in hippocampus, PFC, striatum, and cerebellum (brain areas important for learning and memory showing high DAGL-α activity) (Baggelaar et al., 2017).

Materials and Methods

Animals. Subjects consisted of adult male C57BL/6J mice (The Jackson Laboratory), and *DAGL-α*$^{-/-}$, *DAGL-α*$^{+/-}$, and *DAGL-α*$^{+/+}$ mice on a mixed 99% C57BL/6 (30% J, 70% N) and 1% 129/SvEv background, as previously described (Hsu et al., 2012). *DAGL-α*$^{+/-}$ mouse breeding pairs were originally generated in the B.F.C. laboratory and transferred to Virginia Commonwealth University. All mice (age 8–10 weeks) were pair-housed under a 12 h light/12 h dark cycle (0600 to 1800 h), at a constant temperature (22°C) and humidity (50%–60%), with food and water available *ad libitum*. All experiments were conducted in accordance with the National Institutes of Health *Guide for the care and use of laboratory animals* (Publication No. 8023, revised 1978), and were approved by the Virginia Commonwealth University and Medical College of Wisconsin Institutional Animal Care and Use Committees.

Electrophysiology. For LTP experiments, *DAGL-α*$^{+/+}$, *DAGL-α*$^{+/-}$, *DAGL-α*$^{-/-}$, and *C57BL/6J* mice were anesthetized under isoflurane inhalation and decapitated. Hippocampi were dissected in C57BL/6J mice 2 h after vehicle (VEH), DAGL-α inhibitor DO34 (30 mg/kg, B.F.C. laboratory), or its control analog and ABHD6 inhibitor DO53 (30 mg/kg administration) and were embedded in low-melting-point agarose (3%, Sigma-Aldrich, A0701). Transverse hippocampal slices (400 μm thick) were prepared using a vibrating slicer (Leica Microsystems, VT1200s) (Pan et al., 2011; Zhang et al., 2015). Slices were prepared at 4°C-6°C in a solution containing the following (in mM): 68 sucrose, 2.5 KCl, 1.25 NaH_2PO_4, 5 $MgSO_4$, 26 $NaHCO_3$, and 25 glucose. The slices were transferred to and stored in aCSF containing the following (in mM): 119 NaCl, 3 KCl, 2 $CaCl_2$, 1 $MgCl_2$, 1.25 NaH_2PO_4, 25 $NaHCO_3$, and 10 glucose at room temperature for at least 1 h before use. All solutions were saturated with 95% O_2 and 5% CO_2.

fEPSPs were recorded with patch-clamp amplifiers (Multiclamp 700B) under infrared-differential interference contrast microscopy. The recordings were made blind to drug treatment and mouse genotype. Data acquisition and analysis were performed using digitizers (Digidata 1440A and Digidata 1550B) and the analysis software pClamp 10 (Molecular Devices). Signals were filtered at 2 kHz and sampled at 10 kHz. Field recordings were made using glass pipettes filled with 1 M NaCl (1–2 MΩ) placed in the stratum radiatum of the CA1 region of the hippocampal slices, and fEPSPs were evoked by stimulating the Schaffer collateral/commissural pathway at 0.033 Hz with a bipolar tungsten electrode (WPI). Stable baseline fEPSPs were recorded for at least 20 min at an intensity that induced ~40% of the maximal evoked response. LTP was induced by theta burst stimulation (TBS), which consisted of a series of 15 bursts, with 4 pulses per burst at 100 Hz with a 200 ms interburst interval. TBS is designed to mimic the *in vivo* firing patterns of hippocampal neurons during exploratory behavior (Larson et al., 1986). All recordings were performed at 32 ± 1°C by using an automatic temperature controller.

MWM assessments. The MWM consisted of a circular, galvanized steel tank (1.8 m in diameter, 0.6 m height). The tank was filled with water (maintained at 20 ± 2°C) with a white platform (10 cm diameter) submerged 1 cm below the water's surface. A sufficient volume of white paint (Valspar 4000 latex paint) was added to render the water opaque and the platform invisible. In addition to distal visual cues (shapes) on curtains surrounding the tank (30 cm from the tank wall), five sheets of laminated paper with distinct black-and-white geometric designs were attached to the sides of the tank serving as proximal cues. An automated tracking system (ANY-maze, San Diego Instruments) analyzed the swim path of each subject and calculated distance (path length between being placed in the water and finding the hidden platform), average swim speed, number of platform crossings, and percentage of time spent in each quadrant.

To assess MWM acquisition, *DAGL-α*$^{+/+}$, *DAGL-α*$^{+/-}$, and *DAGL-α*$^{-/-}$ mice received 10 Fixed Platform training days (i.e., a submerged

platform remained in the same location across days), and then were assessed for expression of spatial memory on day 11 in a single MWM Fixed Platform Probe Trial (i.e., the submerged platform was removed). C57BL/6J mice received a 2 h pretreatment of the DAGL-α inhibitor DO34 (0.3, 3, and 30 mg/kg) (Wilkerson et al., 2017), or its inactive analog and ABHD6 inhibitor DO53 (30 mg/kg), or VEH on each of 10 Fixed Platform training days. A cued task test assessed sensorimotor/motivational confounds by placing a 10-cm-high black cylinder on the submerged platform and mice were released from the farthest two release points. To assess whether DO34 affects the expression of spatial memory, separate groups of mice were given 10 d of drug-free Fixed Platform training. On day 11, each subject was administered 30 mg/kg DO34 or VEH, and 2 h later underwent a single 2 min MWM Fixed Platform Probe Trial. The extinction of spatial memory was assessed in drug-naive acquisition trained mice, which received injections of 30 mg/kg DO34 or VEH (2 h pretreatment) at 1, 2, 3, 4, and 6 weeks after acquisition, and tested in 2 min probe trials. To assess forgetting, a group of drug-naive acquisition trained mice were administered 30 mg/kg DO34 or VEH on day 11 and then returned to their home cage, given a second injection of 30 mg/kg DO34 or VEH at 6 weeks after acquisition, and 2 h later underwent a 2 min probe trial. Reversal learning and perseverative behavior were assessed in drug-naive acquisition trained mice, which received injections of 30 mg/kg DO34 or VEH (2 h pretreatment) and trained in reversal task trials in which the submerged platform was moved to the opposite side of the tank over 5 d after acquisition, followed by a 2 min drug-free probe trial on day 6 after acquisition.

OL assessments. The OL task is a hippocampal-dependent adaptation of the Object Recognition task (Assini et al., 2009). The apparatus consisted of a clear acrylic plastic enclosure (40 × 40 × 40 cm) located inside a white sound attenuating box (59 × 52 × 72 cm) with black geometric shapes (stripes vs circles) on two opposing box walls. A red light illuminated each component of this task. For all experiments, mice received 1 h acclimatization to the testing room, and then were placed in the OL apparatus, without objects, to explore freely for 10 min across 2 habituation days (separated by 24 h). An OL trial consisted of two phases (sample and choice) separated by 3 h (see Fig. 7*A*). During the sample phase, mice were placed in the chamber for 10 min, with two identical objects placed on opposing corners of the same box wall. After the 3 h retention delay, each subject was returned to the apparatus for a 2 min choice test, in which one object was moved to the opposite side of the chamber (left and right objects counterbalanced across trials). During pharmacological assessment of DAGL-α inhibition, 30 mg/kg DO34 was administered intraperitoneally 2 h before the sample phase (see Fig. 7*E*). An automated tracking system (ANY-maze, San Diego Instruments) video recorded exploration, and each trial was subsequently scored blind for sample and choice phase object exploration. Exploration of an object was defined as directing the nose to the object at a distance of <2 cm and/or touching it with the nose.

Lipid extraction and mass spectrometry. DAGL-$\alpha^{+/+}$, *DAGL-$\alpha^{+/-}$*, *DAGL-$\alpha^{-/-}$* mice, and *C57BL/6J* mice receiving a 2 or 24 h pretreatment of DO34 (30 mg/kg) or VEH, were anesthetized under isoflurane inhalation and decapitated. Hippocampi, PFC, striatum, and cerebellum were dissected out from brain, flash frozen in liquid nitrogen, and stored at −80°C until assay. On the day of lipid extraction, as previously described (Kwilasz et al., 2014), the preweighed mouse brains were homogenized with 1.4 ml chloroform:methanol (containing 0.0348 g PMSF/ml). Six-point calibration curves ranged from 0.078 to 10 pmol for anandamide (AEA), 0.125–16 nmol for 2-AG, arachidonic acid (AA), and 1-stearoyl-2-arachidonoyl-sn-glycerol, a negative control and blank control were also prepared. Internal standards (Cayman Chemicals) (50 μl of each of 8 nmol SAG-d8, 1 pmol AEA-d8, 1 nmol 2-AG-d8, 1 nmol AA-d8) were added to each calibrator, control, and sample, except the blank control. Each calibrator, control, and sample was then mixed with 0.3 ml of 0.73% w/v NaCl, vortexed, and centrifuged (10 min at 4000 × *g* and 4°C). The aqueous phase plus debris were collected and extracted again twice with 0.8 ml chloroform, the organic phases were pooled, and organic solvents were evaporated under nitrogen gas. Dried samples were reconstituted with 0.1 ml chloroform, mixed with 1 ml cold acetone, and centrifuged (10 min at 4000 × *g* and 4°C) to precipitate proteins. The upper layer of each sample was collected and evaporated to dryness and reconstituted with 0.1 ml methanol and placed in autosample vials for analysis.

An ultra performance liquid chromatography-tandem mass spectrometer was used to identify and quantify the DAGL-α substrate SAG, a nuclear diacyglycerol (Deacon et al., 2002), preferentially used by DAGLs (Balsinde et al., 1991; Allen et al., 1992), the DAGL-α metabolites 2-AG and AA, and AEA, a biosynthetically distinct endogenous cannabinoid ligand, in brain. Sciex 6500 QTRAP system with an IonDrive Turbo V source for TurbolonSpray attached to a Shimadzu ultra performance liquid chromatography system controlled by Analyst Software. Chromatographic separation was performed on a Discovery HS C18 Column 15 cm × 2.1 mm, 3 μm (Supelco), kept at 25°C with an injection volume of 10 μl. The mobile phase consisted of A: acetonitrile and B: water with 1 g/L ammonium acetate and 0.1% formic acid. The following gradient was used: 0.0–2.4 min at 40% A, 2.5–6.0 min at 40% A, hold for 2.1 min at 40% A, then 8.1–9 min 100% A, hold at 100% A for 3.1 min, and return to 40% A at 12.1 min with a flow rate of 1.0 ml/min. The source temperature was set at 600°C and had a curtain gas at a flow rate of 30 ml/min. The ion-spray voltage was 5000 V with ion source gases 1 and 2 flow rates of 60 and 50 ml/min, respectively. The mass spectrometer was run in positive ionization mode for AEA and 2-AG and in negative ionization mode for AA, and the acquisition mode used was multiple reaction monitoring. The following transition ions (*m*/*z*) were monitored with their corresponding collection energies (eV) in parentheses: AEA: 348 > 62 (13) and 348 > 91 (60); AEA-d8: 356 > 63 (13); 2-AG: 379 > 287 (26) and 379 > 296 (28); 2-AG-d8: 384 > 287 (26); AA: 303 > 259 (−25) and 303 > 59 (−60); AA-d8: 311 > 267 (−25). The total run time for the analytical method was 14 min. Chromatographic analysis of SAG was performed on a Hypersil Gold 3 × 50 mm, 5 μ column (Thermo Fisher Scientific), kept at 25°C with an injection volume of 2 μl. The mobile phase consisted 10:90 mM ammonium formate:methanol mobile with a flow rate of 0.5 ml/min. The source temperature, curtain gas at a flow rate, ion-spray voltage, and source gas flow rates were the same as indicated above. The mass spectrometer was run in positive ionization mode. The following transition ions (*m*/*z*) were monitored with their corresponding collection energies (eV) in parentheses: SAG: 646 > 341 (34) and 646 > 287 (38); SAG-d8: 654 > 341 (34). The total run time for the analytical method was 5 min. Calibration curves were analyzed with each analytical batch for each analyte. A linear regression ratio of the peak area analyte counts with the corresponding deuterated internal standard versus concentration was used to construct the calibration curves.

Experimental design and statistical analysis. Electrophysiological data are presented as mean ± SEM. The magnitude of LTP (%) was calculated as follows: 100 × [mean fEPSP slope during the final 10 min of recording/mean baseline fEPSP slope]. Post-tetanic potentiation (PTP) was calculated as the magnitude of the fEPSP slope relative to baseline for the first 5 min after TBS. Results were analyzed with one-way ANOVA followed by Tukey's *post hoc* analysis.

Behavioral data are presented as mean ± SEM. All MWM acquisition, extinction, forgetting, reversal, perseveration and swim speed data, and OL sample phase percentage exploration were analyzed using a mixed-factor ANOVA (distance, percentage time in outer ring, and centimeter/second measures). All probe trial analyses focused on the first minute of exploration, with all gene deletion measures analyzed by one-way ANOVA and Sidak *post hoc* test, and DO34 measures analyzed by independent-groups *t* test. All MWM cued task data were analyzed by one-way ANOVA. MWM swim path selection metrics were assigned per Wagner et al. (2013) into three categories; spatial (direct, indirect, and self-orienting), nonspatial (scanning, circling, and random), and thigmotaxic, and were analyzed for gene deletion using a χ^2 analysis with pairwise comparisons and Bonferroni corrections (MacDonald and Gardner, 2000), and for drug treatments using a Kruskal–Wallis analysis. All OL sample phase total exploration and choice phase measures were analyzed for gene deletion using a one-way ANOVA, and drug studies using independent-groups *t* tests. The discrimination ratio was calculated by dividing the difference in time spent exploring the novel location object and familiar location object by the total object exploration during the 2 min choice phase. From the sample sizes, power was calculated

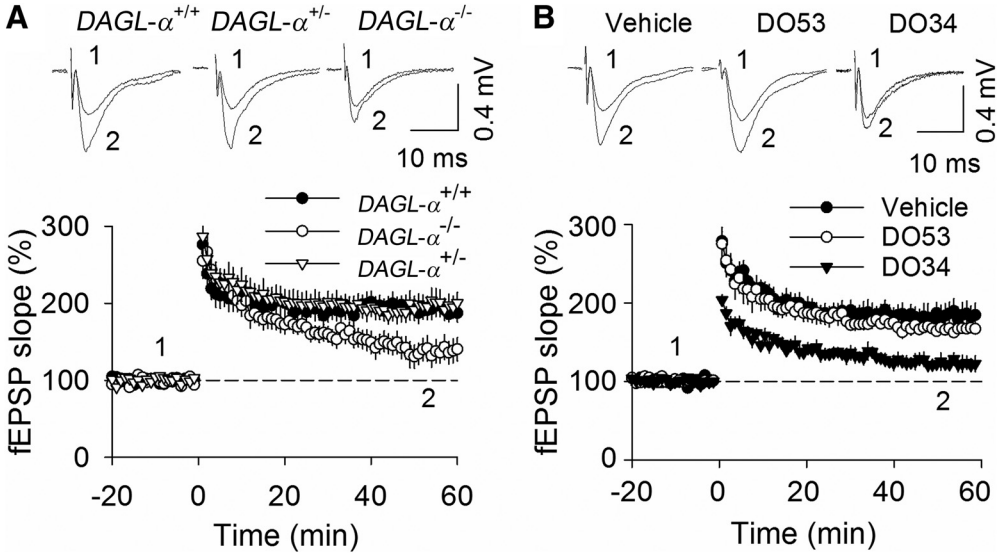

Figure 1. *DAGL-α*$^{-/-}$ mice and C57BL/6 mice treated with the DAGL inhibitor DO34 show disrupted TBS-induced LTP in CA1 of the hippocampus. The magnitude of LTP was significantly decreased in both (***A***) *DAGL-α*$^{-/-}$ mice ($n = 8$) compared with *DAGL-α*$^{+/+}$ ($n = 9$) and *DAGL-α*$^{+/-}$ mice ($n = 11$), as well as in slices from (***B***) DO34-treated C57BL/6J mice ($n = 7$) compared with VEH-treated ($n = 9$) or DO53-treated mice ($n = 8$). The magnitude of PTP during the initial induction phase was also significantly decreased in the DO34 group compared with VEH or DO53. Data are mean ± SEM.

using G*power 3 (Faul et al., 2007) and was found, with α at 0.05, to range from 0.67 to 0.84 for mixed-factor ANOVAs, from 0.45 to 0.99 for one-way ANOVAs, and from 0.34 to 0.51 for independent-group *t* tests.

Before data analysis, brain-level data were transformed to picomoles/gram of brain tissue for AEA, and nanomoles/gram of brain tissue for SAG, 2-AG and AA, and AEA. Drug and gene manipulations on brain endocannabinoids were evaluated by one-way ANOVA, for each lipid in each brain area, followed by a Sidak *post hoc* test. The criterion for significance in all experiments was set at $p < 0.05$, and all analyses were conducted using SPSS Statistics 22 for Windows (IBM).

Results

Experiment 1: genetic deletion or pharmacological blockade of DAGL-α attenuates LTP in CA1 region of the hippocampus

In hippocampal slices prepared from *DAGL-α*$^{+/+}$ and *DAGL-α*$^{+/-}$ mice ($n = 9$–11), TBS induced robust LTP that remained stable during the 60 min recording period (Fig. 1*A*). The fEPSP slope in hippocampal slices from DAGL-α$^{-/-}$ mice ($n = 8$) subjected to the same TBS stimulation slowly decayed toward baseline. The magnitude of LTP as measured between 50 and 60 min after TBS stimulation significantly differed among the three groups ($F_{(2,27)} = 5.37$, $p = 0.011$, ANOVA). *Post hoc* analyses indicated that TBS-induced LTP was significantly greater in *DAGL-α*$^{+/+}$ and *DAGL-α*$^{+/-}$ mice than in *DAGL-α*$^{-/-}$ mice (*DAGL-α*$^{+/+}$ vs *DAGL-α*$^{-/-}$, $p = 0.039$; *DAGL-α*$^{+/-}$ vs *DAGL-α*$^{-/-}$, $p = 0.013$). However, the magnitude of LTP did not differ between *DAGL-α*$^{+/+}$ mice and *DAGL-α*$^{+/-}$ mice ($p = 0.926$).

Hippocampal slices from C57BL/6J mice treated with VEH, DO34 (30 mg/kg), or DO53 (30 mg/kg) showed significant differences in the magnitude of LTP ($F_{(2,23)} = 7.90$, $p = 0.003$, ANOVA; Fig. 1*B*). *Post hoc* tests indicated that TBS induced similar LTP in hippocampal slices prepared from VEH-treated ($n = 9$) and DO53-treated mice ($n = 8$; $p = 0.514$ vs VEH), but slices prepared from DO34-treated mice displayed a significantly decreased magnitude of LTP ($n = 7$; $p = 0.002$ vs VEH; $p = 0.031$ vs DO53). Moreover, the magnitude of PTP during the first 5 min of LTP induction significantly differed among the three treatment groups ($F_{(2,23)} = 7.17$, $p = 0.004$, ANOVA), in which DO34 administration produced a significant decrease in the PTP compared with VEH ($p = 0.007$) and DO53 ($p = 0.011$).

Experiment 2.1: *DAGL-α*$^{-/-}$ mice display profound phenotypic MWM spatial memory deficits and altered MWM search strategies

Per the experimental timeline (Fig. 2*A*), the first acquisition day of Fixed Platform training (data not shown) yielded no significant differences among groups and across trials ($F_{(6,114)} = 1.67$, $p = 0.135$, ANOVA). However, across the 10 days of MWM Fixed Platform acquisition training (Fig. 2*B*), a significant interaction ($F_{(18,342)} = 2.48$, $p = 0.001$, ANOVA) revealed that *DAGL-α*$^{-/-}$ mice ($n = 13$) had longer distances to the platform than *DAGL-α*$^{+/+}$ ($n = 15$) or *DAGL-α*$^{+/-}$ mice ($n = 15$) on acquisition days 2 ($p = 0.001$, $p = 0.005$), 3 ($p = 0.000$, $p = 0.000$), 4 ($p = 0.000$, $p = 0.000$), 5 ($p = 0.000$, $p = 0.000$), 6 ($p = 0.000$, $p = 0.000$), 7 ($p = 0.000$, $p = 0.001$), 8 ($p = 0.001$), 9 ($p = 0.000$, $p = 0.001$), and 10 ($p = 0.000$, $p = 0.000$), respectively. Also, *DAGL-α*$^{+/+}$ mice and *DAGL-α*$^{+/-}$ mice, showed respective significant reductions in distances to the platform on days 4 ($p = 0.005$, $p = 0.014$), 5 ($p = 0.000$, $p = 0.025$), 6 ($p = 0.001$, $p = 0.004$), 7 ($p = 0.000$, $p = 0.000$), 8 ($\alpha^{+/+}$; $p = 0.000$), 9 ($p = 0.000$, $p = 0.007$), and 10 ($p = 0.000$, $p = 0.001$) compared with day 1. In contrast, *DAGL-α*$^{-/-}$ mice showed no significant difference in distance compared with day 1 across subsequent Fixed Platform acquisition days (2; $p = 1.000$, 3; $p = 1.000$, 4; $p = 1.000$, 5; $p = 1.000$, 6; $p = 1.000$, 7; $p = 0.625$, 8; $p = 0.399$, 9; $p = 0.373$, and 10; $p = 0.0670$). Furthermore, during the Fixed Platform probe trial (Fig. 2*C–E*), *DAGL-α*$^{-/-}$ mice demonstrated significantly longer distances to the platform location ($F_{(2,38)} = 5.81$, $p = 0.006$, ANOVA) than *DAGL-α*$^{+/+}$ mice ($p = 0.022$) and *DAGL-α*$^{+/-}$ mice ($p = 0.011$), significantly fewer platform entries ($F_{(2,38)} = 7.40$, $p = 0.002$, ANOVA) than *DAGL-α*$^{+/+}$ mice ($p = 0.001$), and a lower spatial preference for the target quadrant ($F_{(2,38)} = 7.73$, $p = 0.002$, ANOVA) than *DAGL-α*$^{+/+}$ mice ($p = 0.002$) and *DAGL-α*$^{+/-}$ mice ($p = 0.016$). The absence of phenotypic deficits in cued task performance (Fig. 2*F*; $F_{(2,38)} = 0.926$, $p =$

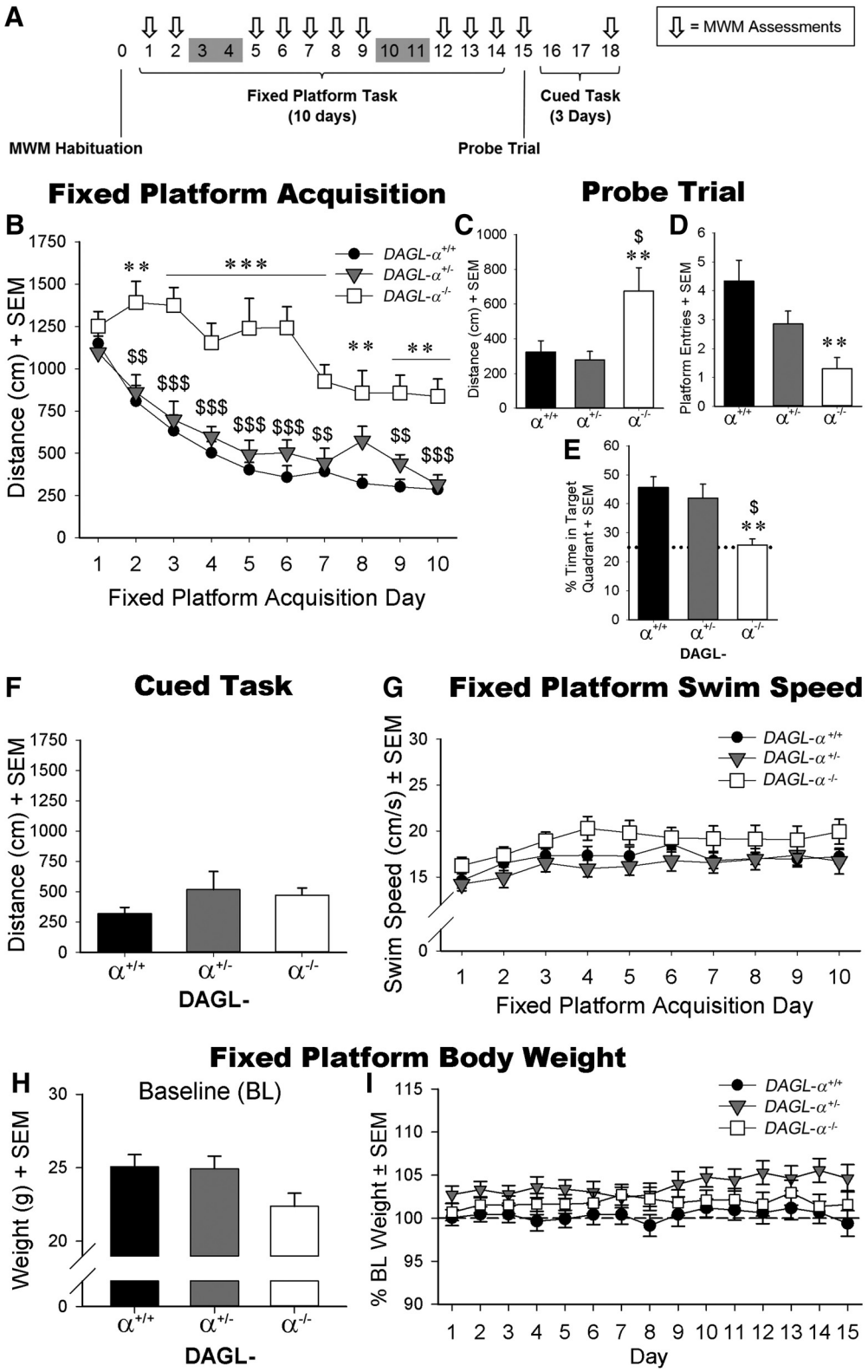

Figure 2. *DAGL-α*$^{-/-}$ mice are profoundly impaired in MWM Fixed Platform task performance. ***A***, Fixed Platform task experimental timeline (days). ***B***, During MWM Fixed Platform acquisition, DAGL-$\alpha^{-/-}$ mice ($n = 13$) exhibited longer distances to the platform than both *DAGL-α*$^{+/+}$ mice ($n = 15$) and *DAGL-α*$^{+/-}$ mice ($n = 13$), as well as showed probe trial performance deficits of (***C***) longer distances to the prior platform position, (***D***) fewer platform entries, and (***E***) a lower spatial preference for the target quadrant. No significant difference in (***F***) cued task performance or (***G***) swim speed suggests that the *DAGL-α*$^{-/-}$ mice performance deficits were unaffected by sensorimotor or motivational impairments. No significant differences were evident in body weight at either (***H***) baseline or (***I***) during Fixed Platform acquisition. Data are mean ± SEM. $^{**}p < 0.01$ versus DAGL-$\alpha^{+/+}$ mice. $^{***}p < 0.001$ versus *DAGL-α*$^{+/+}$ mice. $^{\$}p < 0.05$ versus *DAGL-α*$^{+/-}$ mice. $^{\$\$}p < 0.01$ versus *DAGL-α*$^{+/-}$ mice. $^{\$\$\$}p < 0.001$ versus *DAGL-α*$^{+/-}$ mice.

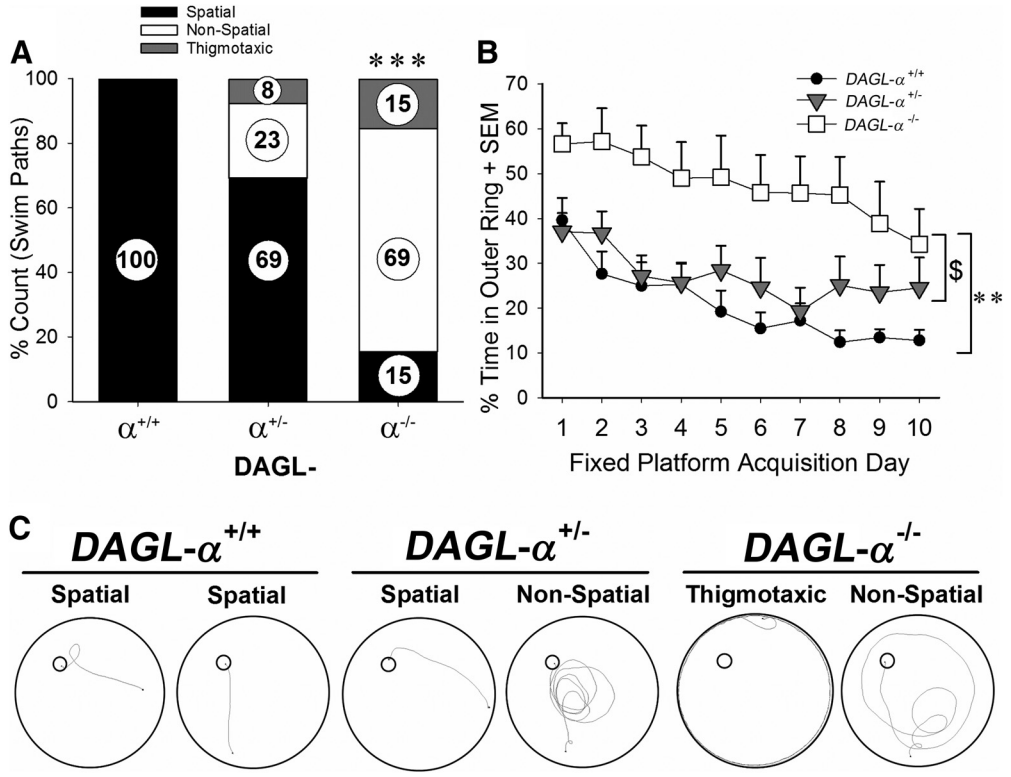

Figure 3. *DAGL-α*$^{-/-}$ mice exhibit altered MWM search strategy. *DAGL-α*$^{-/-}$ mice ($n = 13$) (***A***) used more nonspatial and thigmotaxic swim paths than *DAGL-α*$^{+/+}$ mice ($n = 15$) on Fixed Platform day 10 and (***B***) spent more time in the MWM outer ring than both *DAGL-α*$^{+/+}$ and *DAGL-α*$^{+/-}$ mice ($n = 13$) during Fixed Platform acquisition. ***C***, Fixed Platform day 10 representative swim traces show spatial (direct and self-orienting) swim paths in *DAGL-α*$^{+/+}$ mice, spatial (direct) and nonspatial (circling) swim paths in *DAGL-α*$^{+/-}$ mice, and nonspatial (circling and thigmotaxic) swim paths in *DAGL-α*$^{-/-}$ mice. Data are mean ± SEM. $^{**}p < 0.01$ versus *DAGL-α*$^{+/+}$ mice. $^{***}p < 0.001$ versus *DAGL-α*$^{+/+}$ mice. $^{\$}p < 0.05$ versus *DAGL-α*$^{+/-}$ mice.

0.405, ANOVA) and no alterations in swim speed (Fig. 2*G*; $F_{(18,342)} = 0.648$, $p = 0.860$, ANOVA) suggest that neither sensorimotor nor motivational impairments contribute to the impaired Fixed Platform acquisition of *DAGL-α*$^{-/-}$ mice. Also, no significant differences in body weight at baseline ($F_{(2,38)} = 3.08$, $p = 0.057$, ANOVA; Fig. 2*H*) or during Fixed Platform acquisition ($F_{(2,38)} = 2.84$, $p = 0.071$, ANOVA; Fig. 2*I*) were evident among the genotypes.

On Fixed Platform day 10 (Fig. 3*A*), *DAGL-α*$^{-/-}$ mice used significantly more nonspatial and thigmotaxic swimming strategies than *DAGL-α*$^{+/+}$ or *DAGL-α*$^{+/-}$ mice ($\chi^2_{(4,\,N\,=\,41)} = 21.9$, $p = 0.000$, χ^2). The change in *DAGL-α*$^{-/-}$ mice strategy proportion was indicated by pairwise comparisons ($p = 0.001$). Furthermore, during Fixed Platform acquisition (Fig. 3*B*), a significant main effect of genotype ($F_{(2,38)} = 7.29$, $p = 0.002$, ANOVA) indicated that *DAGL-α*$^{-/-}$ mice spent more time in the MWM outer ring than *DAGL-α*$^{+/+}$ mice ($p = 0.002$) and *DAGL-α*$^{+/-}$ mice ($p = 0.028$). A significant main effect of day ($F_{(9,342)} = 13.9$, $p = 0.000$, ANOVA) also showed that collectively *DAGL-α*$^{+/+}$, *DAGL-α*$^{+/-}$, and *DAGL-α*$^{-/-}$ mice spent a decreased proportion of their time in the outer ring on days 4 ($p = 0.015$), 5 ($p = 0.034$), 6 ($p = 0.001$), and 7–10 ($p = 0.000$) compared with day 1.

Experiment 2.2: pharmacological inhibition of DAGL-α delays MWM spatial acquisition

Per the experimental timeline (Fig. 4*A*), Fixed Platform day 1 (data not shown) yielded no significant differences among groups and across trials ($F_{(12,171)} = 1.65$, $p = 0.082$, ANOVA). During MWM Fixed Platform acquisition (Fig. 4*B*), a significant main effect of drug ($F_{(4,57)} = 8.77$, $p = 0.000$) revealed that 30 mg/kg DO34-treated mice ($n = 12$) required longer swim path distances to the platform than mice in the VEH ($n = 15$, $p = 0.000$), 0.3 mg/kg DO34 ($n = 12$, $p = 0.002$), and 30 mg/kg DO53 ($n = 12$, $p = 0.000$) conditions. However, these mice did not statistically differ from mice receiving 3 mg/kg DO34 ($n = 11$, $p = 0.103$). Also, mice treated with VEH ($F_{(9,126)} = 12.7$, $p < 0.001$, repeated-measures ANOVA), 30 mg/kg DO34 ($F_{(9,99)} = 12.3$, $p = 0.000$, repeated-measures ANOVA), 3 mg/kg DO34 ($F_{(9,90)} = 8.01$, $p = 0.000$, repeated-measures ANOVA), 0.3 mg/kg DO34 ($F_{(9,99)} = 8.48$, $p = 0.000$, repeated-measures ANOVA), and 30 mg/kg DO53 ($F_{(9,99)} = 15.8$, $p = 0.000$, repeated-measures ANOVA) showed significantly reduced distances to the platform days 3 (VEH $p = 0.022$), 4 (VEH $p = 0.000$), 5 (VEH $p = 0.005$; 30 mg/kg DO34 $p = 0.021$; 3 mg/kg DO34 $p = 0.019$; 30 mg/kg DO53 $p = 0.005$), 6 (VEH $p = 0.001$; 30 mg/kg DO34 $p = 0.004$; DO53 $p = 0.003$), 7 (VEH $p < 0.001$; 30 mg/kg DO34 $p = 0.003$; 3 mg/kg DO34 $p = 0.008$; DO53 $p = 0.002$), 8 (VEH $p = 0.003$; 30 mg/kg DO34 $p = 0.034$; 3 mg/kg DO34 $p = 0.038$; DO53 $p = 0.001$), 9 (VEH $p = 0.001$; 30 mg/kg DO34 $p = 0.000$; 3 mg/kg DO34 $p = 0.002$; DO53 $p = 0.000$), and 10 (VEH $p = 0.000$; 30 mg/kg DO34 $p = 0.000$; 3 mg/kg DO34 $p = 0.024$; 0.3 mg/kg DO34 $p = 0.011$; DO53 $p = 0.000$) compared with day 1.

To test whether DO34 affects memory of the platform location (Fig. 4*C*), a probe trial revealed similar distances to the platform location ($t_{(15)} = 0.0880$, $p = 0.931$, independent *t* test; Fig. 4*D*) in DO34-treated and VEH-treated mice, similar number of platform entries ($t_{(15)} = 1.17$, $p = 0.260$, independent *t* test; Fig. 4*E*), and similar percentages of time spent in the target quadrant ($t_{(15)} = 1.28$, $p = 0.220$, independent *t* test; Fig. 4*F*). The absence

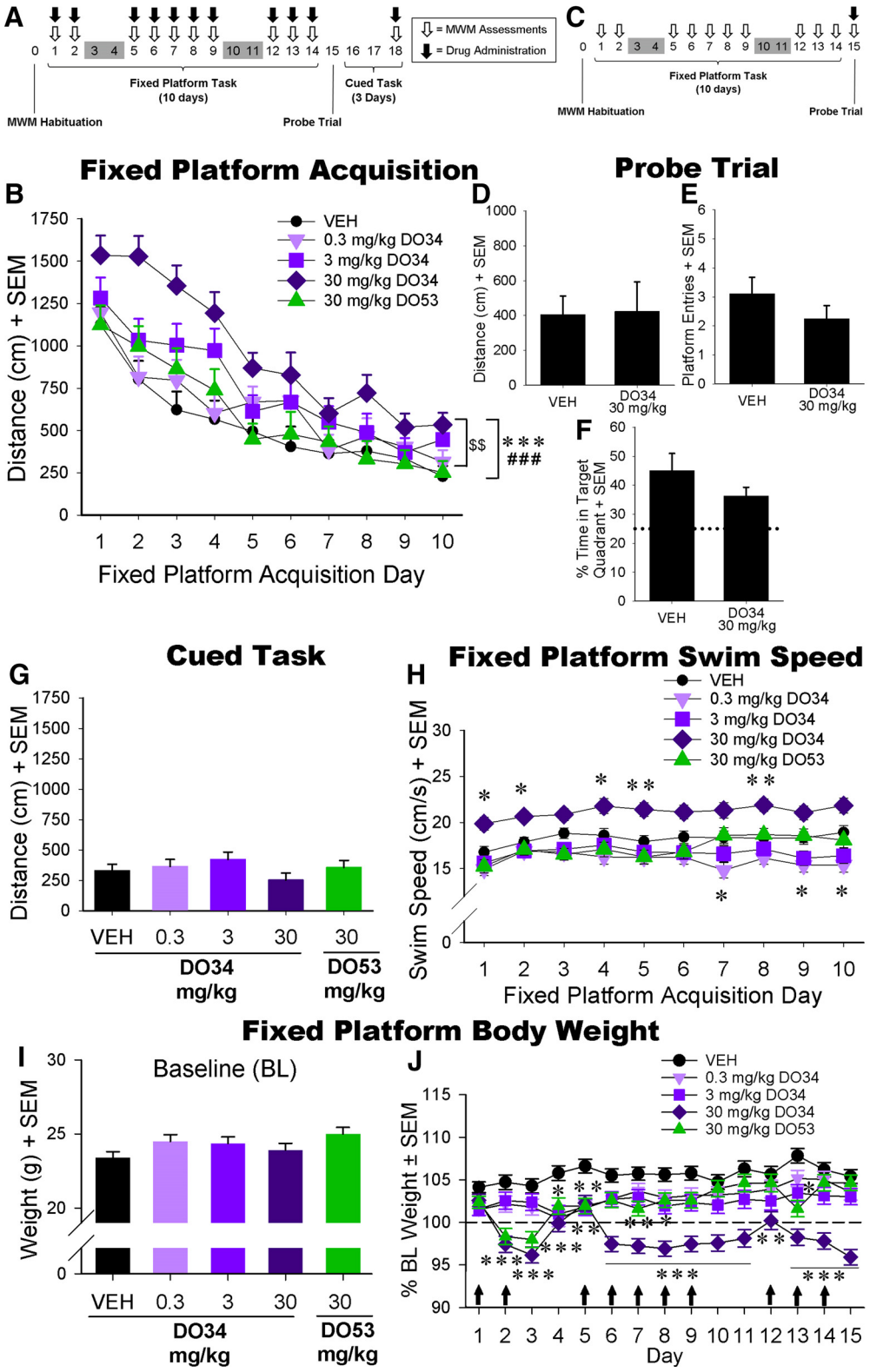

Figure 4. DO34 delays MWM Fixed Platform acquisition but does not affect probe trial performance. ***A***, Fixed Platform task acquisition experimental timeline (days). ***B***, During MWM Fixed Platform acquisition, mice treated with 30 mg/kg DO34 ($n = 12$) exhibited longer distances to the platform than VEH ($n = 15$), 0.3 mg/kg DO34 ($n = 12$), and 30 mg/kg DO53 ($n = 12$). ***C***, Fixed Platform task probe trial (expression) experimental timeline (days). Following drug-free MWM Fixed Platform acquisition training, no change in performance was seen at probe trial between drug treatments (VEH $n = 9$; or 30 mg/kg DO34 $n = 8$) for any measure, (***D***) distances to the prior platform position, (***E***) platform entries, or (***F***) spatial preference for the target quadrant. No difference in (***G***) cued task performance suggests that the high-dose DO34 did not affect sensorimotor or motivational components of MWM performance. ***H***, Mice administered 30 mg/kg DO34 showed increased swim speeds during Fixed Platform acquisition compared with VEH-treated mice on days 1, 2, 4, 5, and 8, but 0.3 mg/kg DO34 reduced swim speeds on days 7, 9, and 10. No significant differences were evident between groups on Fixed Platform training day 1 across trials (data not shown), or in body weight at (***I***) baseline, yet a significant interaction between drug and day on body weight throughout (***J***) acquisition training showed reductions compared with VEH at 30 mg/kg DO34 (days 2–15), 3 mg/kg DO34 (days 4, 8, 13), 0.3 mg/kg DO34 (day 4), and 30 mg/kg DO53 (days 2, 3, 4, 5, 7, 13). Data are mean ± SEM. $^{*}p < 0.05$ versus VEH. $^{**}p < 0.01$ versus VEH. $^{***}p < 0.001$ versus VEH. $^{\$\$}p < 0.01$ versus 0.3 mg/kg DO34. $^{\#\#\#}p < 0.01$ versus 30 mg/kg DO53.

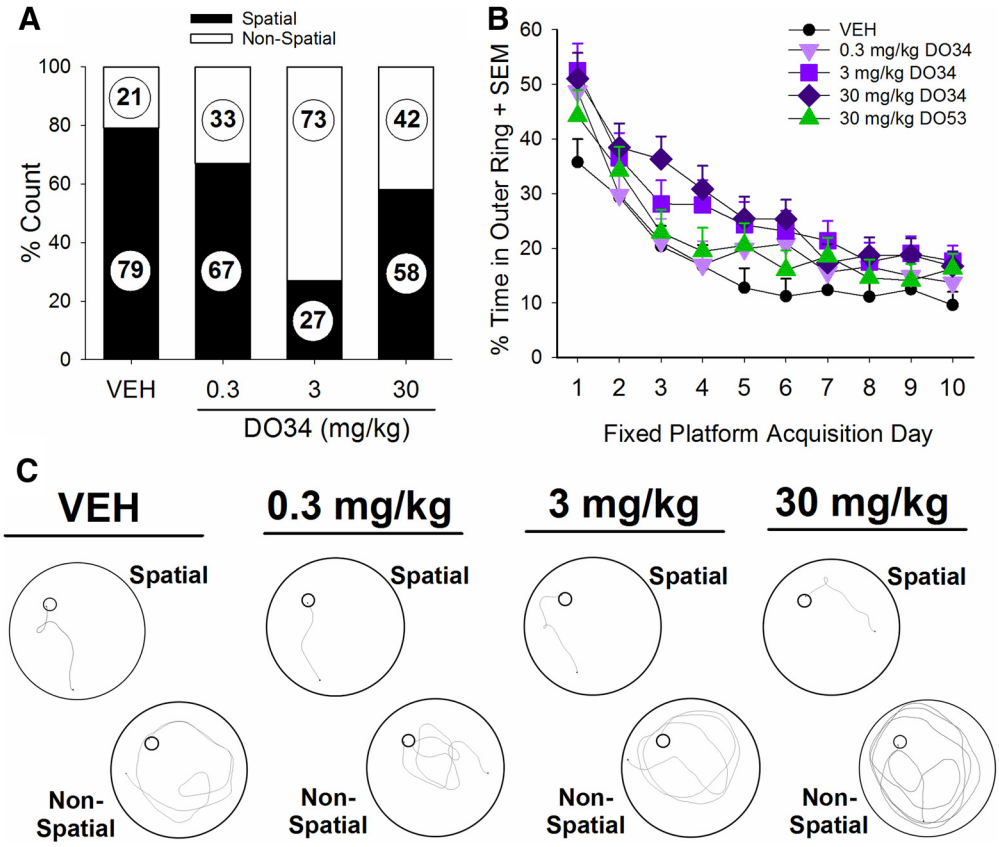

Figure 5. DO34 produces modest and selective changes to MWM search strategy. DO34-treated mice (0.3 mg/kg, $n = 12$; 3 mg/kg, $n = 11$; 30 mg/kg, $n = 12$) (***A***) showed no significant change in swim path strategy than VEH-treated mice ($n = 15$) on Fixed Platform day 10, but (***B***) mice administered 30 mg/kg DO34 showed a modest increase in the time spent in the MWM outer ring during Fixed Platform acquisition than VEH-treated mice. ***C***, Fixed Platform day 10 representative swim traces show spatial (self-orienting and direct) and nonspatial (circling and scanning) swim paths in VEH, and DO34-treated (0.3, 3, 30 mg/kg) mice. Data are mean ± SEM. $p < 0.05$ DO34 (30 mg/kg) versus VEH-treated mice.

of drug-induced deficits in cued task performance ($F_{(4,57)} = 1.09$, $p = 0.368$, ANOVA; Fig. 4*G*) suggests that DO34 does not elicit sensorimotor or motivational impairments.

During Fixed Platform acquisition, a significant swim speed interaction ($F_{(36,513)} = 1.60$, $p = 0.016$, ANOVA; Fig. 4*H*), revealed that mice administered 30 mg/kg DO34 swam faster than VEH-treated mice on days 1 ($p = 0.019$), 2 ($p = 0.010$), 4 ($p = 0.042$), 5 ($p = 0.009$), and 8 ($p = 0.003$), but 0.3 mg/kg DO34-treated mice swam slower than VEH-treated mice on days 7 ($p = 0.026$), 9 ($p = 0.044$), and 10 ($p = 0.022$). Also, while no significant difference in body weight was evident at baseline ($F_{(4,57)} = 2.03$, $p = 0.103$, ANOVA; Fig. 4*I*), a significant interaction between drug and day for this measure occurred throughout acquisition training ($F_{(56,798)} = 7.06$, $p = 0.000$, ANOVA; Fig. 4*J*). DO34 elicited body weight reductions compared with VEH at 30 mg/kg DO34 (days 2–15, $p = 0.000$), 3 mg/kg DO34 (days 4, $p = 0.006$; 8, $p = 0.032$; and 13, $p = 0.015$), 0.3 mg/kg DO34 (day 4, $p = 0.001$), and 30 mg/kg DO53 (days 2, $p = 0.000$; 3, $p = 0.000$; days 4, $p = 0.041$; 5, $p = 0.003$; 7, $p = 0.008$; and 13, $p = 0.000$).

On Fixed Platform day 10, DO34-treated mice showed no significant alterations in swim path strategy ($\chi^2_{(3,\ N\ =\ 49)} = 7.0;97$, $p = 0.069$, χ^2; Fig. 5*A*). However, a significant main effect of drug was found for time spent in the outer ring of the MWM throughout the 10 acquisition sessions ($F_{(4,57)} = 2.96$, $p = 0.027$, ANOVA; Fig. 5*B*). DO34 (30 mg/kg) produced a modest increase in the time spent in the MWM outer ring compared with VEH-treated mice ($p = 0.035$). A significant main effect of day ($F_{(9,513)} = 59.4$, $p = 0.000$, ANOVA) also showed that mice spent a smaller proportion of their time in the outer ring on all subsequent days, 2, 3, 4, 5, 6, 7, 8, 9, and 10 ($p < 0.001$) than on day 1.

Experiment 2.3: pharmacological inhibition of DAGL-α impairs MWM reversal, but not extinction

The next experiments examined the effects of DO34 (30 mg/kg; $n = 8$) versus VEH ($n = 9$) on extinction (Fig. 6*A*), forgetting (Fig. 6*B*), reversal learning, and perseveration (Fig. 7*A*; 30 mg/kg; $n = 15$, VEH; $n = 15$). As shown in Figure 6*C*, repeated exposures to the MWM with removal of the hidden platform following Fixed Platform acquisition day 10 led to increased swim paths regardless of drug treatment ($F_{(5,75)} = 3.08$, $p = 0.014$, ANOVA). Subjects had significantly longer distances to the previous platform location on extinction weeks 4 ($p = 0.047$) and 6 ($p = 0.027$) compared with probe trial. The lack of a statistical interaction between drug and day ($F_{(5,75)} = 0.292$, $p = 0.916$, ANOVA) and lack of significant main effect of drug ($F_{(1,15)} = 1.98$, $p = 0.180$, ANOVA) indicate that DO34 did not affect extinction. In the probe trial assessment of forgetting (Fig. 6*C*), the lack of a statistically significant interaction between drug and day ($F_{(1,10)} = 0.638$, $p = 0.443$, ANOVA) or a main effect of drug ($F_{(1,10)} = 2.50$, $p = 0.145$, ANOVA) indicates that DO34 did not impact forgetting performance.

In the evaluation of reversal learning (Fig. 7*B*), a statistically significant interaction between drug and day ($F_{(5,140)} = 4.43$, $p = 0.001$, ANOVA) indicates that DO34 delayed reversal acquisition. Specifically, DO34 increased swim distances compared with VEH on days 1 ($p = 0.007$), 2 ($p = 0.007$), and 5 ($p = 0.016$). Yet,

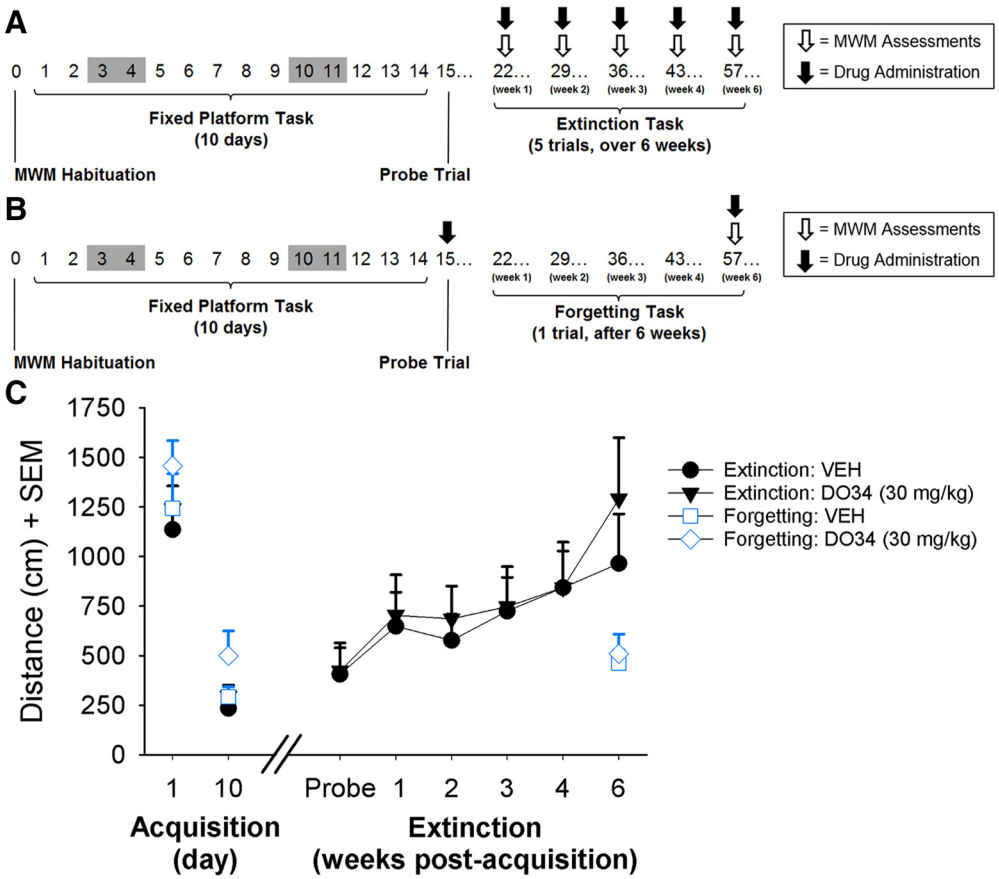

Figure 6. DO34 does not affect extinction or forgetting tasks. ***A***, Experimental timeline for the extinction (days/weeks) of mice trained drug-free in Fixed Platform task (same cohort as per probe trial [expression]; Fig. 4). ***B***, Experimental timeline for additional mice trained drug-free in Fixed Platform task before a forgetting task (days/weeks). ***C***, No change in either the extinction of the Fixed Platform task, or forgetting performance, was seen between VEH ($n = 9$ and $n = 6$, respectively) and 30 mg/kg DO34-treated mice ($n = 8$ and $n = 6$, respectively) (MWM Fixed Platform acquisition day 1 and 10 of VEH and 30 mg/kg DO34 for both extinction and forgetting tasks included for comparison). Data are mean ± SEM.

all subjects displayed evidence of reversal learning after exposure to five reversal sessions (and probe trial) via a main effect of day in VEH ($F_{(5,70)} = 6.05$, $p = 0.000$, repeated-measures ANOVA) and DO34 ($F_{(5,70)} = 13$, $p = 0.000$, repeated-measures ANOVA) mice. VEH-treated subjects had significantly reduced distances to the new platform location on reversal days 2 ($p = 0.011$), 3 ($p = 0.0005$), and 5 ($p = 0.000$) compared with day 1. Similarly, DO34-treated subjects showed reduced swim distances to the platform location on days 2 ($p = 0.033$), 3 ($p = 0.000$), 4 ($p = 0.008$), and 5 ($p = 0.010$) as well as during the probe trial ($p = 0.001$) compared with day 1. Figure 7*C* depicts the percentage of time spent in the quadrant containing the prior platform location. There was no statistical interaction between drug and day ($F_{(4,112)} = 0.498$, $p = 0.737$, ANOVA), but significant main effects of drug ($F_{(1,28)} = 10.29$, $p = 0.003$, ANOVA) and day ($F_{(4,112)} = 34.63$, $p = 0.000$, ANOVA) were found. Further analysis showed that DO34-treated mice ($F_{(4,56)} = 15.72$, $p = 0.000$) spent decreased proportions of time in the quadrant containing the prior platform location on days 2, 3, 4, and 5 (day 2; $p < 0.020$, day 3; $p < 0.009$, day 4; $p < 0.000$, day 5; $p < 0.006$) compared with day 1. These results demonstrate that, although DO34 increased the percentage of time mice spent in the quadrant containing the prior platform location compared with VEH throughout reversal training, mice showed a decrease in the percentage of time in the quadrant containing the prior platform location on days, 2, 3, 4, and 5 ($p < 0.000$) compared with day 1 regardless of drug treatment. Figure 7*D* depicts the percentage of time spent in the quadrant containing the new platform location. Similar to the data in Figure 7*C*, there was no statistical interaction between drug and day ($F_{(4,112)} = 1.34$, $p = 0.260$, ANOVA), but significant main effects of drug ($F_{(1,28)} = 7.37$, $p = 0.011$, ANOVA) and day ($F_{(4,112)} = 28.37$, $p = 0.000$, ANOVA) were found. Although DO34 delayed the magnitude of spatial preference for the quadrant containing the new platform location compared with VEH, it did not affect their spending an increased proportion of their time in the quadrant containing the new platform location on days 2, 3, 4, and 5 (day 2; $p < 0.004$, days 3 to 5; $p < 0.000$) compared with day 1.

Experiment 2.4: the OL task reveals a dissociation of spatial memory deficits between pharmacological inhibition and genetic deletion of DAGL-α

During the sample phase, *DAGL*-$\alpha^{+/+}$ ($n = 13$), *DAGL*-$\alpha^{+/-}$ ($n = 15$), and *DAGL*-$\alpha^{-/-}$ ($n = 7$) mice showed similar total exploration times ($F_{(2,32)} = 2.59$, $p = 0.091$, ANOVA; Fig. 8*B*). None of the genotypes showed a preference for either object (preassigned stationary or moved) ($F_{(2,32)} = 1.61$, $p = 0.22$, ANOVA; Fig. 8*C*). During the choice phase, a significant effect in the discrimination ratio was detected ($F_{(2,32)} = 4.58$, $p = 0.018$, ANOVA; Fig. 8*D*) in which *DAGL*-$\alpha^{-/-}$ ($p = 0.049$) and *DAGL*-$\alpha^{+/-}$ ($p = 0.042$) mice showed significant spatial memory deficits compared with *DAGL*-$\alpha^{+/+}$ mice.

In the evaluation of DO34 on OL spatial memory, sample phase DO34 treatment ($n = 15$) lowered the total exploration

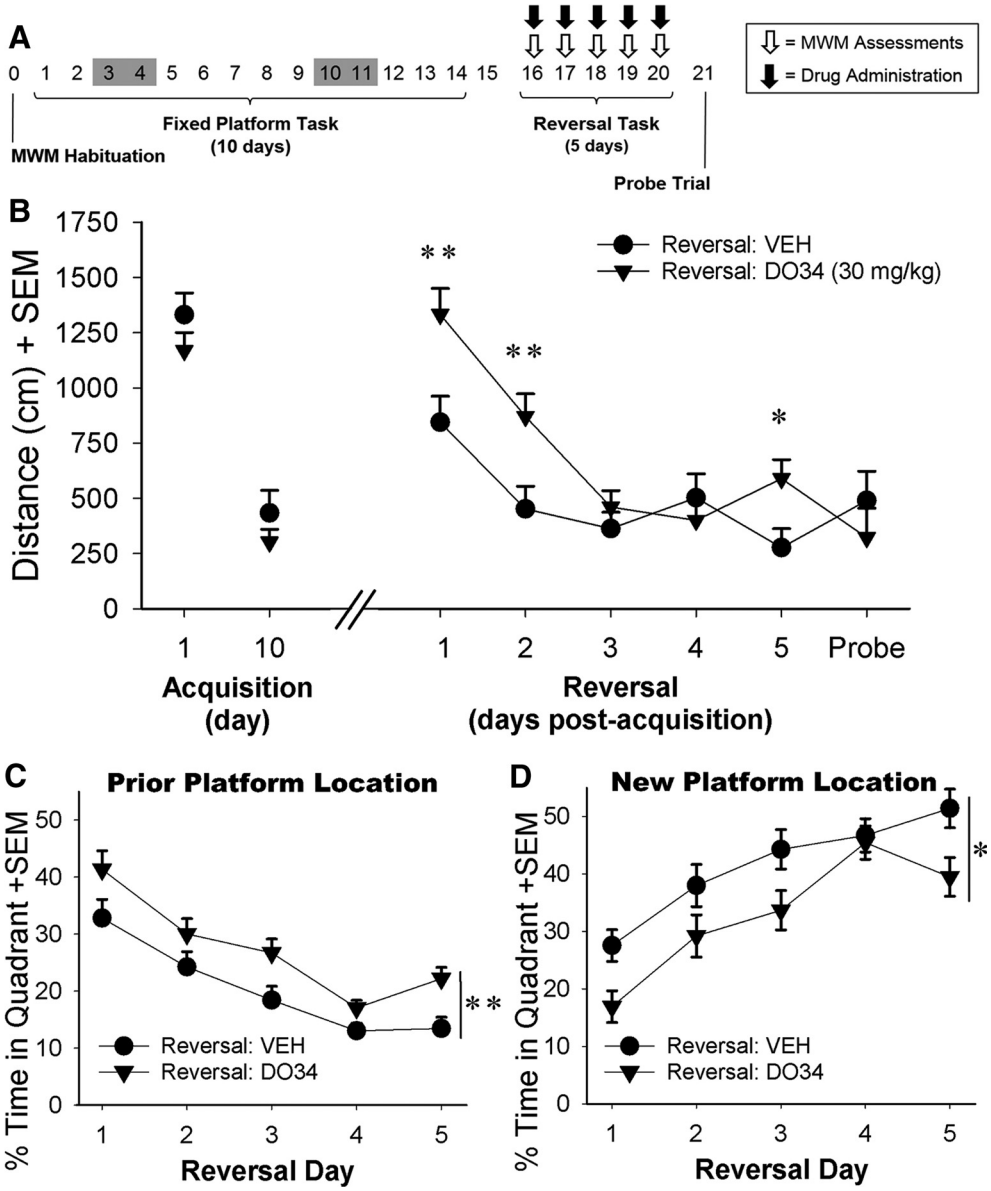

Figure 7. DO34 delays MWM reversal learning but does not produce perseverative behavior. ***A***, Experimental timeline for mice trained in a reversal task (days) following drug-free Fixed Platform training. ***B***, During MWM reversal, mice treated with 30 mg/kg DO34 ($n = 15$) exhibited longer distances to the platform than VEH ($n = 15$) on reversal days 1, 2, and 5 (MWM Fixed Platform acquisition day 1 and 10 of VEH and 30 mg/kg DO34 included for comparison). ***C***, During the same MWM reversal trials, mice treated with 30 mg/kg DO34 also exhibited a delayed inhibition of spatial preference for the quadrant containing the previous platform location compared with VEH. ***D***, During the same MWM reversal trials, mice treated with 30 mg/kg DO34 also exhibited a delayed acquisition of spatial preference for the quadrant containing the new platform location compared with VEH. Data are mean ± SEM. $^*p < 0.05$, $^{**}p < 0.01$.

time compared with VEH ($n = 14$) ($t_{(27)} = 2.69$, $p = 0.012$, t test; Fig. 8*F*). However, neither DO34 nor VEH administration produced a preference for either object (preassigned stationary or moved) ($F_{(1,27)} = 2.97$, $p = 0.096$, ANOVA; Fig. 8*G*). During the choice phase, DO34-treated mice and VEH-treated mice demonstrated evidence of spatial memory, with similar discrimination ratios ($t_{(27)} = 0.62$, $p = 0.54$, t test; Fig. 8*H*).

Experiment 3.1: *DAGL-α*$^{-/-}$ mice show profound alterations in brain endocannabinoids and related lipids

DAGL-$\alpha^{-/-}$ mice ($n = 8$) possessed elevated levels of the DAGL-α substrate, SAG, across all four brain regions, hippocampus ($F_{(2,21)} = 174$, $p = 0.000$, ANOVA; Fig. 9*A*), PFC ($F_{(2,21)} = 753$, $p = 0.000$, ANOVA; Fig. 9*B*), striatum ($F_{(2,21)} = 52$, $p = 0.000$, ANOVA; Fig. 9*C*), and cerebellum ($F_{(2,21)} = 32$, $p = 0.000$, ANOVA; Fig. 9*D*), compared with both DAGL-$\alpha^{+/+}$ ($n = 8$, $p = 0.000$) and DAGL-$\alpha^{+/-}$ mice ($n = 8$, $p = 0.000$). DAGL-$\alpha^{-/-}$ mice also showed profound reductions of 2-AG and its metabolite AA, respectively, across each brain region: hippocampus ($F_{(2,21)} = 246$, $p = 0.000$, ANOVA; Fig. 9*E*; $F_{(2,21)} = 156$, $p = 0.000$, ANOVA; Figure 9*M*), PFC ($F_{(2,21)} = 29$, $p = 0.000$, ANOVA; Fig. 9*F*; $F_{(2,21)} = 207$, $p = 0.000$, ANOVA; Figure 9*N*), striatum ($F_{(2,21)} = 48$, $p = 0.000$, ANOVA; Fig. 9*G*; $F_{(2,21)} = 126$, $p = 0.000$, ANOVA; Figure 9*O*), and cerebellum ($F_{(2,21)} = 70$, $p = 0.000$, ANOVA; Fig. 9*H*; $F_{(2,21)} = 155$, $p = 0.000$, ANOVA; Figure 9*P*), compared with both DAGL-$\alpha^{+/+}$ ($p = 0.000$) and DAGL-$\alpha^{+/-}$ mice ($p = 0.000$). DAGL-$\alpha^{+/-}$ mice showed small but significant reductions of 2-AG compared with DAGL-$\alpha^{+/+}$ mice in striatum ($p = 0.04$), hippocampus ($p = 0.002$), and cerebellum ($p < 0.002$). Also, region-selective reductions of AEA were

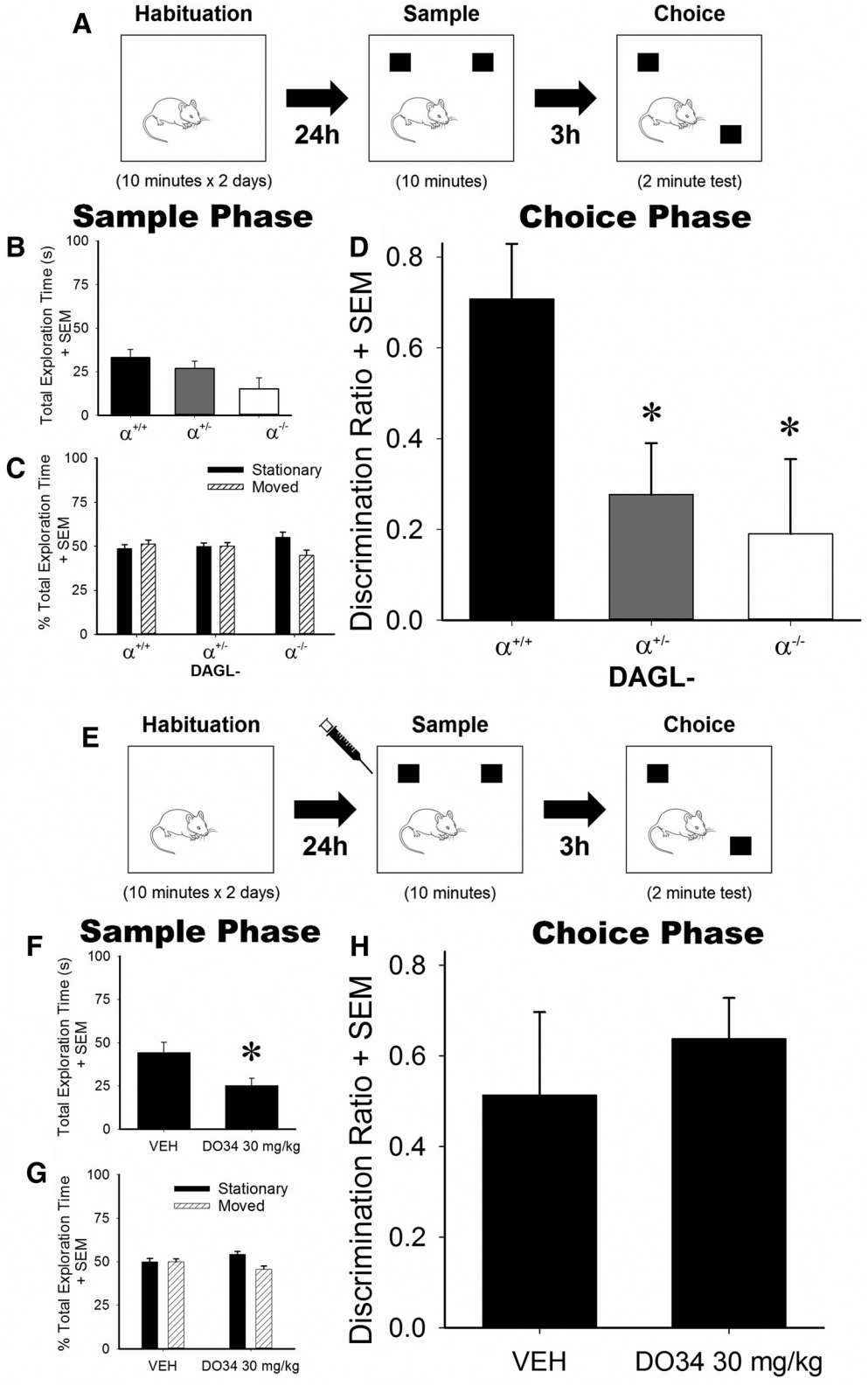

Figure 8. *DAGL-$\alpha^{-/-}$* mice, but not DO34 treated mice, show OL spatial memory deficits. ***A***, Experimental protocol for OL testing of *DAGL-$\alpha^{+/+}$*, *DAGL-$\alpha^{+/-}$*, and *DAGL-$\alpha^{-/-}$* mice. During sample phase, no difference in (***B***) total exploration time (***C***) and no preference for either object (preassigned stationary or moved) were seen between *DAGL-$\alpha^{+/+}$* ($n = 13$), *DAGL-$\alpha^{+/-}$* ($n = 15$), and *DAGL-$\alpha^{-/-}$* ($n = 7$) mice. During choice phase (***D***), a significant decrease in discrimination ratio was evident in *DAGL-$\alpha^{-/-}$* and *DAGL-$\alpha^{+/-}$* mice compared with *DAGL-$\alpha^{+/+}$* mice. ***E***, In the evaluation of DO34 on OL spatial memory, during sample phase (***F***), DO34 treatment ($n = 15$) lowered the total exploration time compared with VEH ($n = 14$), yet (***G***) no preference for either object (preassigned stationary or moved) was seen between DO34 and VEH-treated mice. During choice phase (***H***), DO34 produced no significant change in discrimination ratio compared with VEH-treated mice. Data are mean ± SEM. *$p < 0.05$ versus either *DAGL-$\alpha^{+/+}$* or VEH-treated control mice.

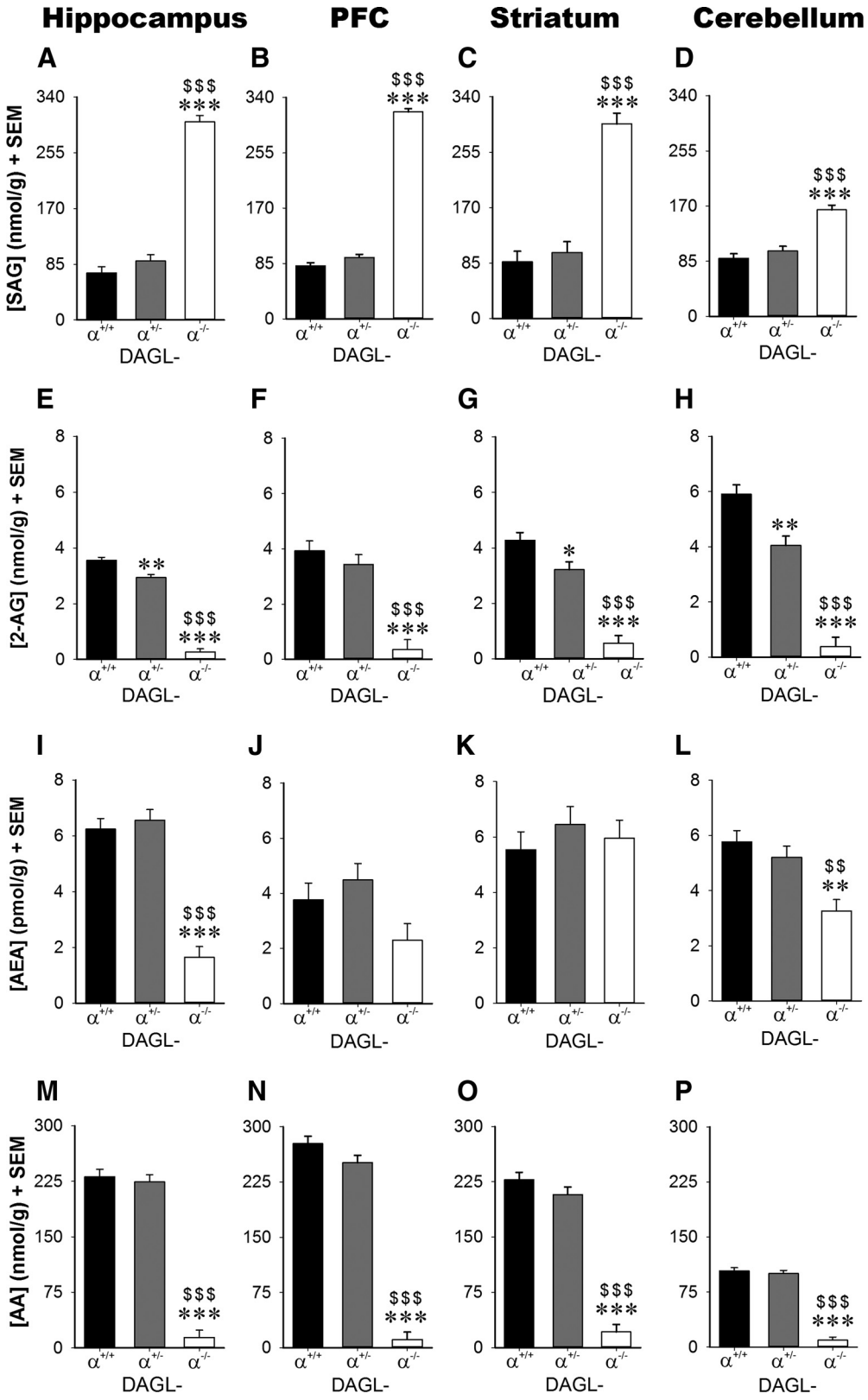

Figure 9. *DAGL-α*$^{-/-}$ mice show profound alterations in brain endocannabinoids. ***A–D***, The DAGL-α substrate SAG was elevated in all four brain regions in *DAGL-α*$^{-/-}$ mice ($n = 8$) compared with both *DAGL-α*$^{+/+}$ ($n = 8$) and *DAGL-α*$^{+/-}$ mice ($n = 8$). *DAGL-α*$^{-/-}$ mice possessed decreased levels of 2-AG and AA, respectively, in (***E***,***M***) hippocampus, (***F***,***N***) PFC, (***G***,***O***) striatum, and (***H***,***P***) cerebellum. *DAGL-α*$^{+/-}$ mice showed modest 2-AG reductions in striatum, hippocampus, and cerebellum compared with *DAGL-α*$^{+/+}$ mice. AEA levels of *DAGL-α*$^{-/-}$ mice were significantly reduced in (***I***) hippocampus and (***L***) cerebellum, but not in (***J***) PFC or (***K***) striatum. Data are mean ± SEM. $^{*}p < 0.05$ versus *DAGL-α*$^{+/+}$ mice. $^{**}p < 0.01$ versus *DAGL-α*$^{+/+}$ mice. $^{***}p < 0.001$ versus *DAGL-α*$^{+/+}$ mice. $^{\$\$}p < 0.01$ versus *DAGL-α*$^{+/-}$ mice. $^{\$\$\$}p < 0.001$ versus *DAGL-α*$^{+/-}$ mice.

found in *DAGL-α*$^{-/-}$ mouse hippocampus ($F_{(2,21)} = 51$, $p = 0.000$, ANOVA; Fig. 9*I*) and cerebellum ($F_{(2,21)} = 10.2$, $p = 0.001$, ANOVA; Fig. 9*L*), but not in PFC (Fig. 9*J*) or striatum (Fig. 9*K*) compared with both *DAGL-α*$^{+/+}$ and *DAGL-α*$^{+/-}$ mice.

Experiment 3.2: DAGL inhibition produces brain region-selective alterations in endocannabinoids and related lipids

DO34-treated mice possessed elevated levels of SAG at 2 h after injection ($n = 5$) across all four brain regions, hippocampus ($F_{(2,15)} = 7.48$, $p = 0.006$, ANOVA; Fig. 10*A*), PFC ($F_{(2,15)} = 30$, $p = 0.000$, ANOVA; Fig. 10*B*), striatum ($F_{(2,15)} = 5.46$, $p = 0.017$, ANOVA; Fig. 10*C*), and cerebellum ($F_{(2,15)} = 6.83$, $p = 0.008$, ANOVA; Fig. 10*D*), compared with VEH ($n = 5$, $p = 0.005$, $p = 0.000$, $p = 0.038$, and $p = 0.006$, respectively). However, at 24 h after injection, SAG levels did not differ between DO34- and VEH-treated mice in each respective brain region ($p = 0.232$, $p = 0.992$, $p = 0.999$, $p = 0.145$). DO34-treated mice also showed consistent reductions of 2-AG in hippocampus ($F_{(2,15)} = 37$, $p = 0.000$, ANOVA; Fig. 10*E*), PFC ($F_{(2,15)} = 11.6$, $p = 0.001$, ANOVA; Fig. 10*F*), striatum ($F_{(2,15)} = 4.82$, $p = 0.024$, ANOVA; Fig. 10*G*), and cerebellum ($F_{(2,15)} = 94$, $p = 0.000$, ANOVA; Fig. 10*H*) at 2 h ($p = 0.000$, $p = 0.001$, $p = 0.036$, and $p = 0.000$, respectively). At 24 h, DO34 continued to decrease 2-AG levels compared with VEH in hippocampus ($p = 0.000$) and cerebellum ($p = 0.000$), but not in PFC or striatum. However, DO34 did not affect AEA levels in hippocampus ($F_{(2,15)} = 0.92$, $p = 0.421$, ANOVA; Fig. 10*I*), PFC ($F_{(2,15)} = 3.04$, $p = 0.078$, ANOVA; Fig. 10*J*), striatum ($F_{(2,15)} = 2.70$, $p = 0.099$, ANOVA; Fig. 10*K*), or cerebellum ($F_{(2,15)} = 2.44$, $p = 0.121$, ANOVA; Fig. 10*L*). Finally, DO34 reduced AA levels in all brain regions: hippocampus ($F_{(2,15)} = 13.8$, $p = 0.000$, ANOVA; Fig. 10*M*) at 2 h ($p = 0.005$) and 24 h ($p = 0.000$), PFC ($F_{(2,15)} = 65$, $p = 0.000$, ANOVA; Fig. 9*N*) at 2 h ($p = 0.000$) and 24 h ($p = 0.000$), striatum ($F_{(2,15)} = 145$, $p = 0.000$, ANOVA; Fig. 9*O*) at 2 h ($p = 0.000$) and 24 h ($p = 0.000$), and cerebellum ($F_{(2,15)} = 59$, $p = 0.000$, ANOVA; Fig. 9*P*) at 2 h ($p = 0.000$) and 24 h ($p = 0.000$). AA levels of DO34-treated mice remained significantly reduced in each brain region at 24 h but were significantly elevated at 24 h compared with 2 h in PFC ($p = 0.000$) and striatum ($p = 0.000$).

Discussion

The present study makes the novel observations that genetic deletion or inhibition of DAGL-α profoundly disrupts hippocampal LTP accompanied with varying magnitudes of spatial learning deficits. Specifically, *DAGL-α*$^{-/-}$ mice display impaired OL and MWM Fixed Platform acquisition accompanied by nonspatial search strategies. Whereas DO34-treated mice show significantly delayed MWM acquisition and reversal learning, performance is spared in probe trial memory, extinction, and forgetting tasks, and in the OL assay. Additionally, these alterations in LTP and *in vivo* learning and memory paradigms occur in concert with distinct altered patterns of endocannabinoids and related lipids, across brain areas integral to learning and memory.

In addition to corroborating a study showing that nonselective DAGL inhibitors block CA1 pairing-induced potentiation in rats (Xu et al., 2012), the present study found significant reductions in hippocampal 2-AG. This pattern of findings in combination with other work showing that inhibitors of 2-AG hydrolysis facilitate CA1 LTP (Silva-Cruz et al., 2017) implicates 2-AG as a possible LTP facilitator. The finding that endogenously produced endocannabinoids facilitate LTP at CA1 hippocampal synapses through stimulation of astrocyte-neuron signaling (Gómez-Gonzalo et al., 2015), or when preceded by DSI (Carlson et al., 2002), suggests that endocannabinoids enhance plasticity by disinhibition. 2-AG acts as a retrograde modulator of short-term CB_1 receptor-mediated synaptic plasticity (i.e., DSE/DSI) (Tanimura et al., 2010; Yoshino et al., 2011). Furthermore, CB_1 receptor activation correlates with enhanced CA1 LTP (Chevaleyre and Castillo, 2004). Thus, reducing 2-AG production may disrupt LTP because of decreased CB_1 receptor signaling. However, the consequences of directly disrupting CB_1 receptor signaling on behavioral performance in hippocampal-dependent learning assays differ from those resulting from DAGL-α disruption. Specifically, WT mice administered a CB_1 receptor antagonist or $CB_1^{-/-}$ mice displayed similar MWM Fixed Platform acquisition as control mice but showed impaired MWM extinction (Varvel and Lichtman, 2002; Varvel et al., 2005). The close spatial localization of DAGL-α to excitatory CB_1 receptor synapses (also adjacent to Group I metabotropic glutamate receptors) and distance from inhibitory synapses (Katona et al., 2006; Yoshida et al., 2006) may account for the resilience of DAGL-α compromised mice in the MWM extinction task.

Contrary to the present work, Sugaya et al. (2013) reported that *DAGL-α*$^{-/-}$ mice show no change in CA1 LTP. As they measured LTP through indwelling electrodes, it is plausible that the altered lipid profile disruption may have interacted with ongoing milieu changes in an awake brain. Thus, procedural differences may account for the different LTP outcomes following DAGL-α deletion. DO34-induced impairment of PTP within minutes of TBS suggests reduced Ca^{2+} buildup in presynaptic axon terminals (Zucker and Regehr, 2002). It is unlikely that DO34 off-targets (e.g., ABDH6) affected the measures, given that DO53 did not affect SC-CA1 LTP. Similarly, DO53 did not alter hippocampal DSI (Ogasawara et al., 2016). As DO34 also inhibits DAGL-β, this 2-AG biosynthetic enzyme cannot be excluded. Yet, its low neuronal expression and high expression on microglia (Hsu et al., 2012) argue against its involvement in the present results.

The phenotypic MWM deficits displayed by *DAGL-α*$^{-/-}$ mice and impaired acquisition and reversal learning performance in DO34-treated mice represent the first evidence supporting a role of DAGL-α in rodent spatial learning and memory models. Specifically, these novel findings indicate that DAGL-α is required for the integration of new spatial information, but not for memory retrieval, extinction, forgetting, or the promotion of perseverative behavior. The findings that DAGL-α deletion profoundly disrupts MWM Fixed Platform learning are compatible with the body of evidence highlighting the necessity of hippocampal neurogenesis for spatial memory processing (Snyder et al., 2005; Sahay et al., 2011), which this enzyme significantly contributes (Goncalves et al., 2008; Gao et al., 2010). DO34-impaired reversal learning is also consistent with chronic stress-induced impairments in MWM reversal learning, which occur concomitantly with lowered hippocampal 2-AG (Hill et al., 2005). Contrary to stress-induced perseveration (Hill et al., 2005), DAGL-α inhibition did not elicit perseverative behavior. Accordingly, this enzyme may be required specifically for integrating new spatial information. The altered search strategy may reflect a stress-induced shift from using hippocampal-cognitive to striatal-habit learning (Wirz et al., 2017). The anxiety-like phenotype of *DAGL-α*$^{-/-}$ mice (Shonesy et al., 2014; Jenniches et al., 2016) as well as the stress-inducing component of the MWM may drive reliance on nonspatial circular search strategies after DAGL-α disruption. Furthermore, elevations in stress hormones (e.g., corticosterone) influence hippocampal-dependent task performance (Kim et al., 2015), al-

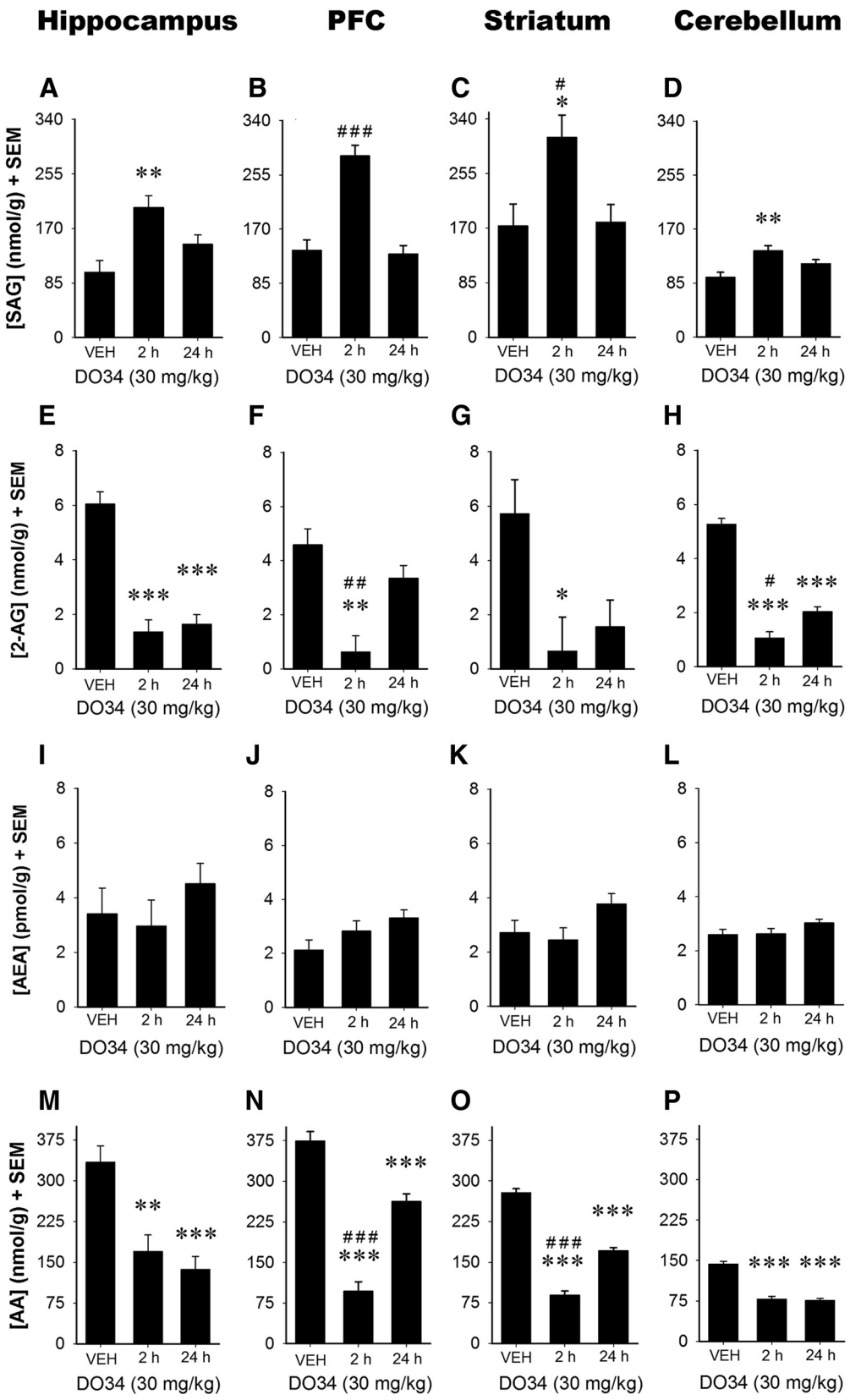

Figure 10. DO34-treated mice show brain region-selective alterations in endocannabinoids and related lipids. ***A–D***, The DAGL-α substrate SAG was elevated in all four brain regions at 2 h after DO34 injection ($n = 5$) compared with VEH ($n = 5$), and compared with 24 h ($n = 8$) in PFC and striatum. At 2 h after DO34 injection, 2-AG and AA were reduced, respectively, in (***E***,***M***) hippocampus, (***F***,***N***) PFC, (***G***,***O***) striatum, and (***H***,***P***) cerebellum. At 24 h after DO34 injection, 2-AG was reduced only in (***E***) hippocampus and (***H***) cerebellum, whereas AA showed reductions across (***M–P***) all four brain areas. No changes in (***I***,***J***,***K***,***L***) AEA were evident compared with VEH. Data are mean ± SEM. $^{*}p < 0.05$ versus VEH. $^{**}p < 0.01$ versus VEH. $^{***}p < 0.001$ versus VEH. $^{\#}p < 0.05$ versus 24 h. $^{\#\#}p < 0.01$ versus 24h. $^{\#\#\#}p < 0.001$ versus 24h.

though additional studies are needed to ascertain whether stress hormones contribute to *DAGL-α*$^{-/-}$ phenotypic deficits in hippocampal-dependent task performance. Contrary to the present findings, extinction, but not acquisition deficits, occur in DO34-treated mice (Cavener et al., 2018) or *DAGL-α*$^{-/-}$ mice (Jenniches et al., 2016; Cavener et al., 2018) in conditioned fear tasks. While DAGL-α is expressed in regions mediating fear conditioning, such as the BLA (Yoshida et al., 2011), stress reduces amygdala-hippocampal connectivity (Wirz et al., 2017). Accordingly, DAGL-α may differentially modulate memory processes based on brain circuitry, region, or neuronal type.

The differential impact between genetic deletion and pharmacological inhibition of DAGL-α on performance in spatial learning tasks may partly be a consequence of 2-AG lipid profile differences. However, developmental alterations in the brains of the *DAGL-α*$^{-/-}$ mice across ontogeny may also be a contributing factor. In the developing brain, DAGL-α is expressed on presynaptic terminals (Bisogno et al., 2003), participating in the control of axonal growth and guidance (Williams et al., 1994; Brittis et al., 1996) but is expressed on postsynaptic neurons in the adult brain. Accordingly, across ontogeny, DAGL-α switches roles from growth and guidance to a modulator of synaptic signaling. The finding that *DAGL-α*$^{-/-}$ mice, but not DO34-treated mice, possessed significantly reduced AEA levels in hippocampus and cerebellum raises the possibility that diminished AEA levels may contribute to the *DAGL-α*$^{-/-}$ phenotypic learning and memory deficits and altered search strategy.

Profound lipid profile changes accompanied the spatial memory impairments of *DAGL-α*$^{-/-}$ mice. As previously reported (Gao et al., 2010; Tanimura et al., 2010; Shonesy et al., 2014; Jenniches et al., 2016), these mice displayed substantial reductions of 2-AG across all four brain areas. In *DAGL-α*$^{+/-}$ mice, modest reductions of 2-AG in striatum, hippocampus, and cerebellum may have contributed to OL deficits, although they displayed similar performance as WT mice in MWM tasks. Whereas previous studies reported DO34-induced 2-AG decreases in whole brain (Ogasawara et al., 2016; Wilkerson et al., 2017), we found reductions of 2-AG in each region evaluated. *DAGL-α*$^{-/-}$ mice showed reductions of AEA in hippocampus and cerebellum, but not in cortex or striatum. Similarly, Tanimura et al. (2010) reported reduced striatal AEA levels, whereas Jenniches et al. (2016) found AEA reductions in cortex and amygdala. DO34 did not affect AEA levels in any brain region investigated, despite 50% reductions of AEA in whole brain (Ogasawara et al., 2016; Wilkerson et al., 2017). Thus, DAGL-α substrates and metabolites appear to play a complex role in AEA biosynthesis. Given that inhibitors of the primary AEA hydrolytic enzyme, fatty acid amide hydrolase (FAAH), impair LTP (Basavarajappa et al., 2014), yet enhance MWM acquisition and extinction (Varvel et al., 2007), the consequences of reduced hippocampal AEA in *DAGL-α*$^{-/-}$ mice must be considered. Examining whether an FAAH inhibitor rescues *DAGL-α*$^{-/-}$ phenotypes may provide insight into whether AEA functionally contributes to the impairments observed in the present study. Nonetheless, it should be noted that a FAAH inhibitor failed to reverse fear extinction deficits in *DAGL-α*$^{-/-}$ mice (Cavener et al., 2018).

The impact of DAGL-α blockade on downstream and upstream lipid signaling molecules, previously only evaluated in forebrain (Shonesy et al., 2014) or whole brain (Ogasawara et al., 2016), merits discussion. The expression of DAGL in invertebrate species lacking cannabinoid receptors (e.g., *Drosophila*) (Elphick and Egertova, 2005) underscores the important role of this enzyme in regulating lipid signaling molecules independent of substrate production for cannabinoid receptor activation. As anticipated, both *DAGL-α*$^{-/-}$ mice and DO34-treated mice showed consistent elevations of the DAG substrate for DAGL-α, SAG, across all four brain areas. SAG activates PKC (Hindenes et al., 2000); and while PKC activation facilitates memory (Bonini et al., 2007), the effects of sustained SAG elevations are not known. The dramatically reduced levels of AA across all four brain regions in *DAGL-α*$^{-/-}$ and DO34-treated mice suggest that DAGL-α is an important intermediate for the maintenance of basal AA levels in brain. Given that hippocampal neurons activate PKC through AA cascades (Hama et al., 2004), the DAGL-α disruption-induced AA reductions may also contribute to the observed learning and memory deficits.

Collectively, this work supports the importance of DAGL-α in modulating hippocampal learning and memory to the extent that reductions in DAGL-α expression or function may contribute to cognitive pathologies. Age-related decreases in DAGL-α expression (Piyanova et al., 2015) suggest that DAGL-α dysregulation may be a useful target for the study of age-related cognitive decline (Bilkei-Gorzo et al., 2017). In sum, the present findings, that DAGL-α disruption led to cellular spatial memory impairments and *in vivo* deficits selective for the integration of new spatial information, implicate this enzyme as playing a key role in spatial learning and memory.

References

Allen AC, Gammon CM, Ousley AH, McCarthy KD, Morell P (1992) Bradykinin stimulates arachidonic acid release through the sequential actions of an sn-1 diacylglycerol lipase and a monoacylglycerol lipase. J Neurochem 58:1130–1139.

Assini FL, Duzzioni M, Takahashi RN (2009) Object location memory in mice: pharmacological validation and further evidence of hippocampal CA1 participation. Behav Brain Res 204:206–211.

Baggelaar MP, van Esbroeck AC, van Rooden EJ, Florea BI, Overkleeft HS, Marsicano G, Chaouloff F, van der Stelt M (2017) Chemical proteomics maps brain region specific activity of endocannabinoid hydrolases. ACS Chem Biol 12:852–861.

Balsinde J, Diez E, Mollinedo F (1991) Arachidonic acid release from diacylglycerol in human neutrophils: translocation of diacylglycerol-deacylating enzyme activities from an intracellular pool to plasma membrane upon cell activation. J Biol Chem 266:15638–15643.

Basavarajappa BS, Nagre NN, Xie S,Subbanna S (2014) Elevation of endogenous anandamide impairs LTP, learning, and memory through CB1 receptor signaling in mice. Hippocampus 24:808–818.

Bilkei-Gorzo A, Albayram O, Draffehn A, Michel K, Piyanova A, Oppenheimer H, Dvir-Ginzberg M, Rácz I, Ulas T, Imbeault S, Bab I, Schultze JL, Zimmer A (2017) A chronic low dose of Δ9-tetrahydrocannabinol (THC) restores cognitive function in old mice. Nat Med 23:782–787.

Bisogno T, Howell F, Williams G, Minassi A, Cascio MG, Ligresti A, Matias I, Schiano-Moriello A, Paul P, Williams EJ, Gangadharan U, Hobbs C, Di Marzo V, Doherty P (2003) Cloning of the first sn1-DAG lipases points to the spatial and temporal regulation of endocannabinoid signaling in the brain. J Cell Biol 163:463–468.

Bonini JS, Da Silva WC, Bevilaqua LR, Medina JH, Izquierdo I, Cammarota M (2007) On the participation of hippocampal PKC in acquisition, consolidation and reconsolidation of spatial memory. Neuroscience 147:37–45.

Brittis P, Silver J, Walsh F, Doherty P (1996) Fibroblast growth factor receptor function is required for the orderly projection of ganglion cell axons in the developing mammalian retina. Mol Cell Neurosci 8:120–128.

Carlson G, Wang Y, Alger BE (2002) Endocannabinoids facilitate the induction of LTP in the hippocampus. Nat Neurosci 5:723–724.

Cavener VS, Gaulden A, Pennipede D, Jagasia P, Uddin J, Marnett LJ, Patel S (2018) Inhibition of diacylglycerol lipase impairs fear extinction in mice. Front Neurosci 12:479.

Chau LY, Tai HH (1981) Release of arachidonate from diglyceride in human platelets requires the sequential action of a diglyceride lipase and a monoglyceride lipase. Biochem Biophys Res Commun 100: 1688–1695.

Chevaleyre V, Castillo PE (2004) Endocannabinoid-mediated metaplasticity in the hippocampus. Neuron 43:871–881.

Deacon EM, Pettitt TR, Webb P, Cross T, Chahal H, Wakelam MJ, Lord JM (2002) Generation of diacylglycerol molecular species through the cell cycle: a role for 1-stearoyl, 2-arachidonyl glycerol in the activation of nuclear protein kinase C-βII at G2/M. J Cell Sci 115:983–989.

Elphick M, Egertova M (2005) The phylogenetic distribution and evolutionary origins of endocannabinoid signalling. Handb Exp Pharmacol 168:283–297.

Faul F, Erdfelder E, Lang AG, Buchner A (2007) G*Power 3: a flexible statistical power analysis program for the social, behavioral, and biomedical sciences. Behav Res Methods 39:175–191.

Gao Y, Vasilyev DV, Goncalves MB, Howell FV, Hobbs C, Reisenberg M, Shen R, Zhang MY, Strassle BW, Lu P, Mark L, Piesla MJ, Deng K, Kouranova EV, Ring RH, Whiteside GT, Bates B, Walsh FS, Williams G, Pangalos MN, et al. (2010) Loss of retrograde endocannabinoid signaling and reduced neurogenesis in diacylglycerol lipase knock-out mice. J Neurosci 30:2017–2024.

Gómez-Gonzalo M, Navarrete M, Perea G, Covelo A, Martín-Fernández M, Shigemoto R, Luján R, Araque A (2015) Endocannabinoids induce lateral long-term potentiation of transmitter release by stimulation of gliotransmission. Cereb Cortex 25:3699–3712.

Goncalves MB, Suetterlin P, Yip P, Molina-Holgado F, Walker DJ, Oudin MJ, Zentar MP, Pollard S, Yáñez-Muñoz RJ, Williams G, Walsh FS, Pangalos MN, Doherty P (2008) A diacylglycerol lipase-CB2 cannabinoid pathway regulates adult subventricular zone neurogenesis in an age-dependent manner. Mol Cell Neurosci 38:526–536.

Hama H, Hara C, Yamaguchi K, Miyawaki A (2004) PKC signaling mediates global enhancement of excitatory synaptogenesis in neurons triggered by local contact with astrocytes. Neuron 41:405–415.

Hill MN, Patel S, Carrier EJ, Rademacher DJ, Ormerod BK, Hillard CJ, Gorzalka BB (2005) Downregulation of endocannabinoid signaling in the hippocampus following chronic unpredictable stress. Neuropsychopharmacology 30:508–515.

Hindenes JO, Nerdal W, Guo W, Di L, Small DM, Holmsen H (2000) Physical properties of the transmembrane signal molecule, sn-1-stearoyl 2-arachidonoylglycerol. J Biol Chem 275:6857–6867.

Hsu KL, Tsuboi K, Adibekian A, Pugh H, Masuda K, Cravatt BF (2012) DAGLβ inhibition perturbs a lipid network involved in macrophage inflammatory responses. Nat Chem Biol 8:999–1007.

Jenniches I, Ternes S, Albayram O, Otte DM, Bach K, Bindila L, Michel K, Lutz B, Bilkei-Gorzo A, Zimmer A (2016) Anxiety, stress, and fear response in mice with reduced endocannabinoid levels. Biol Psychiatry 79: 858–868.

Katona I, Urbán G, Wallace M, Ledent C, Jung KM, Piomelli D, Mackie K, Freund TF (2006) Molecular composition of the endocannabinoid system at glutamatergic synapses. J Neurosci 26:5628–5637.

Kim EJ, Pellman B, Kim JJ (2015) Stress effects on the hippocampus: a critical review. Learn Mem 22:411–416.

Kwilasz AJ, Abdullah RA, Poklis JL, Lichtman AH, Negus SS (2014) Effects of the fatty acid amide hydrolase (FAAH) inhibitor URB597 on pain-stimulated and pain-depressed behavior in rats. Behav Pharmacol 25: 119–129.

Lafourcade M, Elezgarai I, Mato S, Bakiri Y, Grandes P, Manzoni OJ (2007) Molecular components and functions of the endocannabinoid system in mouse prefrontal cortex. PLoS One 2:e709.

Larson J, Wong D, Lynch G (1986) Patterned stimulation at the theta frequency is optimal for the induction of hippocampal long-term potentiation. Brain Res 368:347–350.

Lieberwirth C, Pan Y, Liu Y, Zhang Z, Wang Z (2016) Hippocampal adult neurogenesis: its regulation and potential role in spatial learning and memory. Brain Res 1644:127–140.

MacDonald PL, Gardner RC (2000) Type I error rate comparisons of post hoc procedures for IxJ chi-square tables. Educ Psychol Meas 60:735–754.

Ogasawara D, Deng H, Viader A, Baggelaar MP, Breman A, den Dulk H, van den Nieuwendijk AM, van den Nieuwendijk AM, Soethoudt M, van der Wel T, Zhou J, Overkleeft HS, Sanchez-Alavez M, Mori S, Mo S, Nguyen W, Conti B, Liu X, Chen Y, Liu QS, et al. (2016) Rapid and profound rewiring of brain lipid signaling networks by acute diacyglycerol lipase inhibition. Proc Natl Acad Sci U S A 113:26–33.

Okazaki T, Sagawa N, Okita JR, Bleasdale JE, MacDonald PC, Johnston JM (1981) Diacylglycerol metabolism and arachidonic acid release in human fetal membranes and decidua vera. J Biol Chem 256:7316–7321.

Pan B, Wang W, Zhong P, Blankman JL, Cravatt BF, Liu QS (2011) Alterations of endocannabinoid signaling, synaptic plasticity, learning, and memory in monoacylglycerol lipase knock-out mice. J Neurosci 31: 13420–13430.

Piyanova A, Lomazzo E, Bindila L, Lerner R, Albayram O, Ruhl T, Lutz B, Zimmer A, Bilkei-Gorzo A (2015) Age-related changes in the endocannabinoid system in the mouse hippocampus. Mech Ageing Dev 150: 55–64.

Sahay A, Scobie KN, Hill AS, O'Carroll CM, Kheirbek MA, Burghardt NS, Fenton AA, Dranovsky A, Hen R (2011) Increasing adult hippocampal neurogenesis is sufficient to improve pattern separation. Nature 472: 466–470.

Shonesy BC, Bluett RJ, Ramikie TS, Báldi R, Hermanson DJ, Kingsley PJ, Marnett LJ, Winder DG, Colbran RJ, Patel S (2014) Genetic disruption of 2-arachidonoylglycerol synthesis reveals a key role for endocannbinoid signaling in anxiety modulation. Cell Rep 9:1644–1653.

Silva-Cruz A, Carlström M, Ribeiro JA, Sebastião AM (2017) Dual influence of endocannabinoids on long-term potentiation of synaptic transmission. Front Pharmacol 8:921.

Snyder JS, Hong NS, McDonald RJ, Wojtowicz JM (2005) A role for adult neurogenesis in spatial long-term memory. Neuroscience 130: 843–852.

Sugaya Y, Cagniard B, Yamazaki M, Sakimura K, Kano M (2013) The endocannabinoid 2-arachidonoylglycerol negatively regulates habituation by suppressing excitatory recurrent network activity and reducing long-term potentiation in the dentate gyrus. J Neurosci 33:3588–3601.

Tanimura A, Yamazaki M, Hashimotodani Y, Uchigashima M, Kawata S, Abe M, Kita Y, Hashimoto K, Shimizu T, Watanabe M, Sakimura K, Kano M (2010) The endocannabinoid 2-arachidonoylglycerol produced by diacylglycerol lipase alpha mediates retrograde suppression of synaptic transmission. Neuron 65:320–327.

Varvel SA, Lichtman AH (2002) Evaluation of CB1 receptor knockout mice in the Morris Water Maze. J Pharmacol Exp Ther 301:915–924.

Varvel SA, Anum EA, Lichtman AH (2005) Disruption of CB(1) receptor signaling impairs extinction of spatial memory in mice. Psychopharmacology (Berl) 179:863–872.

Varvel SA, Wise LE, Niyuhire F, Cravatt BF, Lichtman AH (2007) Inhibition of fatty-acid amide hydrolase accelerates acquisition and extinction rates in a spatial memory task. Neuropsychopharmacology 23:1032–1041.

Viader A, Ogasawara D, Joslyn C, Sanchez-Alavez M, Mori S, Nguyen W, Conti B, Cravatt B (2015) A chemical proteomic atlas of brain serine hydrolases identifies cell type-specific pathways regulating neuroinflammation. Elife 5:1–24.

Wagner AK, Brayer SW, Hurwitz M, Niyonkuru C, Zou H, Failla M, Arenth P, Manole MD, Skidmore E, Thiels E (2013) Non-spatial pre-training in the water maze as a clinically relevant model for evaluating learning and memory in experimental TBI. Neurobiol Learn Mem 106:71–86.

Wilkerson JL, Donvito G, Grim TW, Abdullah RA, Ogasawara D, Cravatt BF, Lichtman AH (2017) Investigation of diacylglycerol lipase alpha inhibition in the mouse lipopolysaccharide inflammatory pain model. J Pharmacol Exp Ther 363:394–401.

Williams EJ, Walsh FS, Doherty P (1994) The production of arachidonic acid can account for calcium channel activation in the second messenger pathway underlying neurite outgrowth stimulated by NCAM, N-cadherin, and L1. J Neurochem 62:1231–1234.

Williams EJ, Walsh FS, Doherty P (2003) The FGF receptor uses the endocannabinoid signaling system to couple to an axonal growth response. J Cell Biol 160:481–486.

Wirz L, Reuter M, Felten A, Schwabe L (2017) A haplotype associated with enhanced mineralocorticoid receptor expression facilitates the

stress-induced shift from "cognitive" to "habit" learning. eNeuro 4:ENEURO.0359-17.2017.

Xu JY, Zhang J, Chen C (2012) Long-lasting potentiation of hippocampal synaptic transmission by direct cortical input is mediated via endocannabinoids. J Physiol 590:2305–2315.

Yoshida T, Fukaya M, Uchigashima M, Miura E, Kamiya H, Kano M, Watanabe M (2006) Localization of diacyglycerol lipase-alpha around postsynaptic spine suggests close proximity between production site of an endocannabinoid, 2-arachidonoyl-glycerol, and presynaptic cannabinoid CB1 receptor. J Neurosci 26:4740–4751.

Yoshida T, Uchigashima M, Yamasaki M, Katona I, Yamazaki M, Sakimura K, Kano M, Yoshioka M, Watanabe M (2011) Unique inhibitory synapse with particularly rich endocannabinoid signaling machinery on pyramidal neurons in basal amygdaloid nucleus. Proc Natl Acad Sci U S A 108:3059–3064.

Yoshino H, Miyamae T, Hansen G, Zambrowicz B, Flynn M, Pedicord D, Blat Y, Westphal RS, Zaczek R, Lewis DA, Gonzalez-Burgos G (2011) Postsynaptic diacylglycerol lipase mediates retrograde endocannabinoid suppression of inhibition in mouse prefrontal cortex. J Physiol 589:4857–4884.

Zhang Z, Wang W, Zhong P, Liu SJ, Long JZ, Zhao L, Gao HQ, Cravatt BF, Liu QS (2015) Blockade of 2-arachidonoylglycerol hydrolysis produces antidepressant-like effects and enhances adult hippocampal neurogenesis and synaptic plasticity. Hippocampus 25:16–26.

Zucker RS, Regehr WG (2002) Short-term synaptic plasticity. Annu Rev Physiol 64:355–405.